

DISSERTATION

OPERATION OF ELECTRIC MICROGRIDS UNDER UNCERTAINTY

Submitted by

Mayank Panwar

Department of Electrical and Computer Engineering

In partial fulfillment of the requirements

For the Degree of Doctor of Philosophy

Colorado State University

Fort Collins, Colorado

Spring 2017

Doctoral Committee:

Advisor: Siddharth Suryanarayanan

Sudipta Chakraborty

Rob O. Hovsopian

Peter M. Young

Daniel J. Zimmerle

Copyright by Mayank Panwar 2017

All Rights Reserved

ABSTRACT

OPERATION OF ELECTRIC MICROGRIDS UNDER UNCERTAINTY

Optimization and decision-making are non-trivial in case of multiple, incommensurable, and conflicting objectives. Decision-making becomes more complicated with uncertainty in inputs. Power system operation with electric microgrids subsumes all of the abovementioned aspects. Centralized decision-making in day-ahead dispatch of microgrids with multiple objectives in a grid-connected mode is addressed from the perspective of a power distribution system operator. Uncertainties in the electrical output of variable distributed energy resources and load demand due to forecasting errors are treated statistically by using empirical distributions. Scenarios for simulation are generated using statistics of actual data for solar and load demand forecast. *Kantorovich distance* measure is used for scenario reduction to maintain computational tractability of the problem. Discrete compromise programming is used for multi-criteria decision-analysis to obtain non-dominated dispatch solutions without generating a computationally expensive *Pareto front*. Two step look-ahead dynamic program routine is used for dispatch optimization of dispatchable, non-dispatchable solar, and energy storage asset. New performance metrics are developed for reserve management in microgrids using North American Electric Reliability Corporation (NERC) metrics and some previously developed metrics by this researcher. The economic dispatch problem is formulated as a constrained optimization problem with the new metric for reserve as a constraint. Optimization programs are implemented using MATLAB[®] and power system simulations are performed on standard IEEE 13-node test distribution feeder using the real-time simulation platform—RTDS[®]. Some potential future developments and applications of performance metrics are presented as future work.

ACKNOWLEDGMENTS

The support and guidance from my academic advisor, Prof. Siddharth Suryanarayanan, were of utmost importance for completion of this dissertation. I thank him for advising me through graduate school; especially during the past two years when I was at Idaho National Laboratory (INL) to finish my research work. I would like to thank: Dr. Sudipta Chakraborty at National Renewable Energy Laboratory (NREL) who mentored me in my first year at NREL, and agreed to be on my committee; and Dr. Rob Hovsopian who was my mentor at INL, and also agreed to serve on my committee. Their support was very crucial to continue my research and is duly acknowledged. I would also like to thank Prof. Peter Young, and Prof. Dan Zimmerle for serving on my committee, and Prof. Liuqing Yang for relevant inputs that improved my research.

I would like to acknowledge the financial support: through Alliance Partner University Program (APUP) at NREL (subcontract no. May, 2013 to May, 2014), and through Ph.D. internship under Laboratory Directed Research and Development (LDRD) project (number 15-135) at INL (subcontract number 5-300722 May, 2014 to September, 2016). Administrative support from Electrical and Computer Engineering (ECE) department at Colorado State University is also acknowledged. During the past two years, I also got opportunities to work with various Ph.D. interns at INL—Dr. Julian D. Osorio Ramirez (Florida State University), Ren Liu (Washington State University), and Marija Stevic (RWTH Aachen University) on a variety of research problems. These collaborations have been a good learning experience.

I would like to thank: Anant, Ninad, Vibhanshu, and Hrushikesh for hosting during my frequent visits to Colorado; Aditi, Majid, Akshat, and Svetomir for interesting conversations during breaks; Fathalla, Turk, and other colleagues at APEL and INL. Lastly, I would like to thank my parents for their love and encouragement, and friends in Idaho Falls for their support.

TABLE OF CONTENTS

ABSTRACT	ii
ACKNOWLEDGEMENTS	iii
TABLE OF CONTENTS	iv
LIST OF TABLES	vi
LIST OF FIGURES	vii
NOMENCLATURE	ix
1 INTRODUCTION	1
1.1 Objective, Motivation, and Scope	1
1.2 Contributions of Research	4
1.3 Organization of the Dissertation	5
1.4 Tools and Techniques	6
1.5 Additional Research Work	7
2 MODELING AND VALIDATION OF A DISTRIBUTION FEEDER	8
2.1 Literature Review	8
2.2 Modeling and Validation	22
3 DISPATCH OF MICROGRID ASSETS UNDER UNCERTAINTY	35
3.1 Day-ahead Dispatch under Uncertainty	37
3.2 Simulation Results	52
4 PERFORMANCE METRICS FOR RESERVE MANAGEMENT	64
4.1 Performance Metrics	64
4.2 Application to Reserve Management in Day-ahead Dispatch	67
4.3 Sensitivity Analysis	75

5 CONCLUSIONS AND FUTURE WORK 77

APPENDIX

LIST OF TABLES

Table 1.1	Publications used directly for the preparation of the dissertation.....	5
Table 1.2	Publications for additional research work as part of a contract with INL	7
Table 2.1	Error profile with the variation of the leakage reactance of voltage regulator transformer	28
Table 2.2	Steady-state voltage magnitude and relative error in %	28
Table 2.3	Steady-state phase angle profile and absolute error in degrees	29
Table 3.1	DER ratings and interfaces in the microgrid.....	48
Table 3.2	Empirical distribution statistics (μ, σ) for scenario generation.....	50
Table 3.3	Objective function average values for scenario-based and deterministic dispatch..	56
Table 3.4	MCDA process for selection of dispatch corresponding to minimum cost-to-go function during 17th hour	57
Table 4.1	Data for load demand and solar output	70
Table 4.2	Economic dispatch with various capacity reserve constraints.....	71
Table 4.3	Economic dispatch with R-metric as L.H.S. of reserve constraint (7c).....	72
Table 4.4	Comparison of average dispatch and reserve values	73

LIST OF FIGURES

Figure 1.1	Organization of the dissertation with salient points of the work in each chapter	6
Figure 2.1	Example CHIL simulation	13
Figure 2.2	Example PHIL simulation.....	14
Figure 2.3	Potential role of HIL simulation	20
Figure 2.4	IEEE 13-node distribution test feeder.....	22
Figure 2.5	Error profile for voltage and phase angle with variation of the leakage reactance of voltage regulator transformers	27
Figure 3.1	Flowchart for dispatch using goal attainment and DCP-based MCDA.....	45
Figure 3.2	Illustration of MCDA applied to set of solutions from the multi-objective optimization dispatch problem.....	46
Figure 3.3	Microgrid model using IEEE 13-node feeder and DERs in RSCAD [®] interfaced with dispatch optimization code in MATLAB [®]	48
Figure 3.4	Solar irradiance profile for Ft. Collins, CO and load demand profile used for simulation.....	49
Figure 3.5	Distributions of sampled scenarios for simulations	51
Figure 3.6	Q-Q plots for the original and the reduced scenarios	51
Figure 3.7	Hourly objective function values for stochastic scenarios and preference weights $w = [10, 100, 1]$ during on-peak hours and $w = [1, 1, 10]$ during off-peak hours ...	53
Figure 3.8	Hourly dispatch values for case shown in Fig. 3.7	54
Figure 3.9	Bar chart (stacked) for hourly dispatch values for battery, PV, and diesel generator	55

Figure 4.1	System level representation of various capacity based quantities for one time period	65
Figure 4.2	A bar graph for microgrid operation with microgrid capacity reserve	67
Figure 4.3	Dispatch for Case-7 using R-metric as reserve constraint	72
Figure 4.4	Variation of R-metric as reserve constraint in Case-7	73
Figure 4.5	Sensitivity analysis for R-metric	75

NOMENCLATURE

μ, ν, e	Subscript quantity for microgrid and EPS, respectively
d, nd	Superscript quantity for dispatchable and non-dispatchable DER, respectively
μ, σ	mean and variance of a distribution
c	Total available capacity during an hour
f	Operating cost for dispatchable generator
L	Total load demand during an hour
p	Power output from an asset during an hour
pr	Peak reserve ratio at an hour
r_{cur}	Reliability cost of unused reserve
r_{vur}	Reliability value of unused reserve
w	Reliability metric for asset based on NERC criterion
Δ	Dispatchable reserve during an hour
t_{period}	Number of hours a unit was active in a year
φ	Cost function used in optimization
c_e, c_μ	Cost of generation in \$/kWh for EPS and microgrid
$\alpha_0, \alpha_1, \alpha_2$	Coefficients for diesel cost function
χ_e, χ_μ	Emission factors for EPS and microgrid assets
η_c, η_d	Efficiency for BESS charging, discharging respectively
x_c, x_d	Binary variables denoting BESS charging, discharging respectively
$\tilde{\cdot}$	tilde denotes stochastic variable

γ	scalar to be minimized in goal-attainment programming
ϑ	goals for goal-attainment programming
$soc, \underline{soc}, \overline{soc}$	state-of-charge, state-of-charge lower, and state-of-charge upper limit
p_e, p_μ	Costs of generation outputs in kWh for EPS and microgrid
c_d	Cost of diesel generator operation
F_{max}	Rated fuel usage of diesel generator in gal/h
f_d	Fuel use rate
C_d	Cost of diesel in \$/gal
ϕ	Loading factor of generator in per unit
L_i^p	DCP-based distance metric for i^{th} objective using p^{th} norm
ω	User preference (weight) used in MCDA
w	Weight for an objective during optimization
r	Order of <i>Wasserstein metric</i>
ANSI	American National Standards Institute
APUP	Alliance Partner University Program
BESS	Battery Energy Storage System
CAA	Clean Air Act
CAN	Computer Area Network
CDM	Customer Driven Microgrids
CHIL	Controller Hardware-In-the-Loop
CHP	Combined Heat and Power
CT	Current Transformer
DAE	Differential Algebraic Equations

DAQ	Data Acquisition
DCP	Discrete Compromise Programming
DCS	Distributed Control System
DER	Distributed Energy Resource
DER	Distributed Energy Resource
DM	Decision Maker
DR	Demand Response
DSO	Distribution System Operator
DSS	Decision Support System
ECE	Electrical and Communication Engineering
ED	Economic Dispatch
EMTP	Electro Magnetic Transient Program
EPA	Environmental Protection Agency
EPS	Electric Power System
ESS	Energy Storage System
FCU	Fort Collins Utilities
HIL	Hardware-In-the-Loop
HTS	High Temperature Superconductor
HuT	Hardware under Test
INL	Idaho National Laboratory
IPS	Integrated Power Systems
LDRD	Laboratory Directed Research and Development
MCDA	Multi-Criteria Decision Analysis

NERC	North American Electric Reliability Corporation
NREL	National Renewable Energy Laboratory
O&M	Operation and Maintenance
Opal-RT	Opal-RT is a commercial simulator for real-time EMTP simulations
PHIL	Power Hardware-In-the-Loop
PLR	Peak Load Reduction
PRPA	Platte River Power Authority
PT	Potential Transformer
PV	Photovoltaic
R	Resistance
RSCAD [®]	RTDS [®] Simulator Computer Aided Design software
RT	Real-Time
RTDS [®]	Real Time Digital Simulator
SOC	State-Of-Charge
SSN	State Space Nodal
TCP	Transmission Control Protocol
TNA	Transient Network Analyzer
ToU	Time of Use
VSC	Voltage Source Converter
WACS	Wide Area Control System
X	Reactance
ZIP	Constant-Z (Impedance), -I (Current), -P (Power) composite load

CHAPTER 1

INTRODUCTION

1.1 Objective, Motivation, and Scope

Objective

This work presents a method for multi-objective dispatch of an electric microgrid. Multi-criteria decision-making approach is used for multi-objective dispatch of a microgrid. Performance metrics are developed for systematic inclusion of standard and custom performance measures of each distributed energy resources (DER) in operation of a microgrid. The newly developed metric is applied for reserve management of a microgrid in grid-connected mode. The power system is modeled in a real-time simulation environment using a standard IEEE test distribution feeder. This system is modified by integrating DERs to form a microgrid which is used in power system simulations in RTDS[®].

Motivation

Some of the biggest challenges in DER integrated microgrids are the capital costs, operation and maintenance (O&M) costs, and the operational reliability of the DERs. Scientific and engineering advancement has continually reduced the manufacturing costs of renewable technologies, power electronic interfaces, energy storage, and the integration costs of DERs in the past decade. The operational cost and reliability of microgrids is strongly tied to the dispatch methodology. A dispatch strategy with renewable and dispatchable DERs in microgrids can be challenging, and a trade-off occurs between cost and reliability. Since a microgrid can serve several different purposes, the dispatch philosophy or the trade-off between multiple objectives becomes non-trivial. Hence, an appropriate dispatch framework is required that can handle

multiple traditional and user-defined objectives. The performance of the microgrid must be assessed using metrics to reflect the inherent characteristics of its constituent DERs and to utilize the capacity effectively without high reserves. Operation without high reserves implies that the reliability requirements are met or improved without maintaining high unused capacity of a microgrid as reserves. To address the abovementioned issues, metrics must be developed for a systematic assessment of microgrid operation. Further, the application of these specific metrics in the traditional framework of operation such as economic dispatch, reserve management, and multi-objective dispatch must be developed.

Scope of Research

The scope of the research in this dissertation spans modeling of a typical distribution system integrated with DERs, and a central controller for energy management decisions to form a microgrid. A day-ahead dispatch algorithm is implemented as part of the controller in the dissertation research. Stochastic uncertainty is included in dispatch by using empirical distributions. The research work considers hourly time-scale for data and decisions, and does not address shorter time-scale (< 1 -hour) problems. Although real-time dispatch (5, 10 or 15-minutes) and regulation are interesting problems, the behavior of underlying distribution of stochastic uncertainty, and market operation are different at shorter time-scales than for day-ahead dispatch. Hence, the shorter time-scale problems must be treated separately, and are left for future research. The potential applicability of present research in shorter time-scale operation with possible modifications is presented in Chapter-5. The details and scope are summarized for each area of work in the following sections.

Modeling and Validation of a Distribution Feeder

A comprehensive literature review of the applications of real-time simulation in electric microgrids is presented. The focus is on microgrid related applications. Steady-state modeling and validation is performed in RSCAD[®] (the modeling software with graphical user interface for RTDS[®]) for a standard distribution feeder with typical characteristics of a distribution system with unbalanced loads, single and two phase lines, non-transposed lines, underground cables, unbalanced dynamic ZIP (constant impedance, current, and power) loads, and a voltage regulator. This system is modeled in a real-time simulation environment using components and models suitable for dynamic and transient simulations. DER models for synchronous diesel generator, solar photovoltaic (PV) inverter, and battery energy storage are integrated into the distribution feeder model in a real-time environment, and interfaced with the dispatch algorithm in MATLAB[®] to form a microgrid.

Microgrid Dispatch under Uncertainty

The dispatch algorithm consists of the framework to include multiple objectives and solves a constrained optimization problem by including physical asset-level and system-level constraints. Uncertainties due to forecasting errors of solar irradiance and load demand are included in the dispatch by using empirical distributions. Hourly data from a real-world system are used for the inputs to the simulations. Stochastic scenarios are generated using samples from empirical distributions of solar irradiance and load demand values. Scenario reduction is used for maintaining computational tractability of the problem. The decision maker (DM) has the flexibility to include user-defined objectives or constraints, and also include the preferences of the objectives in the dispatch process. A multi-criteria decision analysis (MCDA) based

approach is used to help the DM choose feasible solutions that are closest to the preferences specified by the DM.

Performance Metrics

Some new performance metrics are developed that combine traditional and previously developed metrics by this researcher to assess the reliability of the microgrid. The characteristics of the constituent DERs are measured through traditional metrics and combined with the new performance metrics to evaluate the reliability-based cost and value of the unused reserves in the microgrid. The reliability-based metric is used as a constraint for reserve management in economic dispatch. Application of the newly developed metric, R-metric, is demonstrated with comparisons to traditional capacity based reserve.

1.2 Contributions of Research

- The modeled test distribution feeder is available as a validated open-source model that can be used for steady-state as well as dynamic power system simulations.
- MCDA-based approach provides a framework for choosing non-dominated solutions without generating a computationally expensive *Pareto front*. This approach can be used in tandem with both exact and heuristic optimization algorithms for dispatch and can include a large number of objectives during dispatch.
- The new performance metrics developed in this work consider traditional NERC metrics and custom performance measures to quantify the reliability-based value of reserve in a microgrid. A systematic procedure to incorporate this new metric is also demonstrated.

1.3 Organization of the Dissertation

The publications prepared as part of research work in this dissertation are listed in Table 1.1. Paper-1 and paper-2 are already peer-reviewed and published, and paper-3 and paper-4 are under review for two peer-reviewed journals at the time of preparation of this dissertation. The work presented in these publications is used in the preparation of the chapters for this dissertation (with appropriate permissions from the copyright holder). The chapters using the content are tabulated with the corresponding publications. Figure 1.1 shows organization of the dissertation.

Table 1.1 Publications used directly for the preparation of the dissertation

S.no.	Paper	Chapter
1.	M. Panwar , B. Lundstrom, J. Langston, S. Suryanarayanan, and S. Chakraborty, “An overview of real time hardware-in-the-loop capabilities in digital simulation for electric microgrids,” in <i>North American Power Symposium (NAPS), 2013</i> , 2013, pp. 1–6.	2
2.	M. Panwar , S. Suryanarayanan, and S. Chakraborty, “Steady-state modeling and simulation of a distribution feeder with distributed energy resources in a real-time digital simulation environment,” in <i>North American Power Symposium (NAPS), 2014</i> , 2014, pp. 1–6.	2
3.	M. Panwar , S. Suryanarayanan, and R. Hovsopian, “A multi-criteria decision analysis-based approach for dispatch of electric microgrids,” in <i>International Journal of Electrical Power and Energy Systems</i> , under review.	3
4.	M. Panwar , S. Suryanarayanan, and R. Hovsopian, “A performance metric for reserve management in day-ahead dispatch of electric microgrids,” in <i>Applied Energy</i> , under preparation.	4

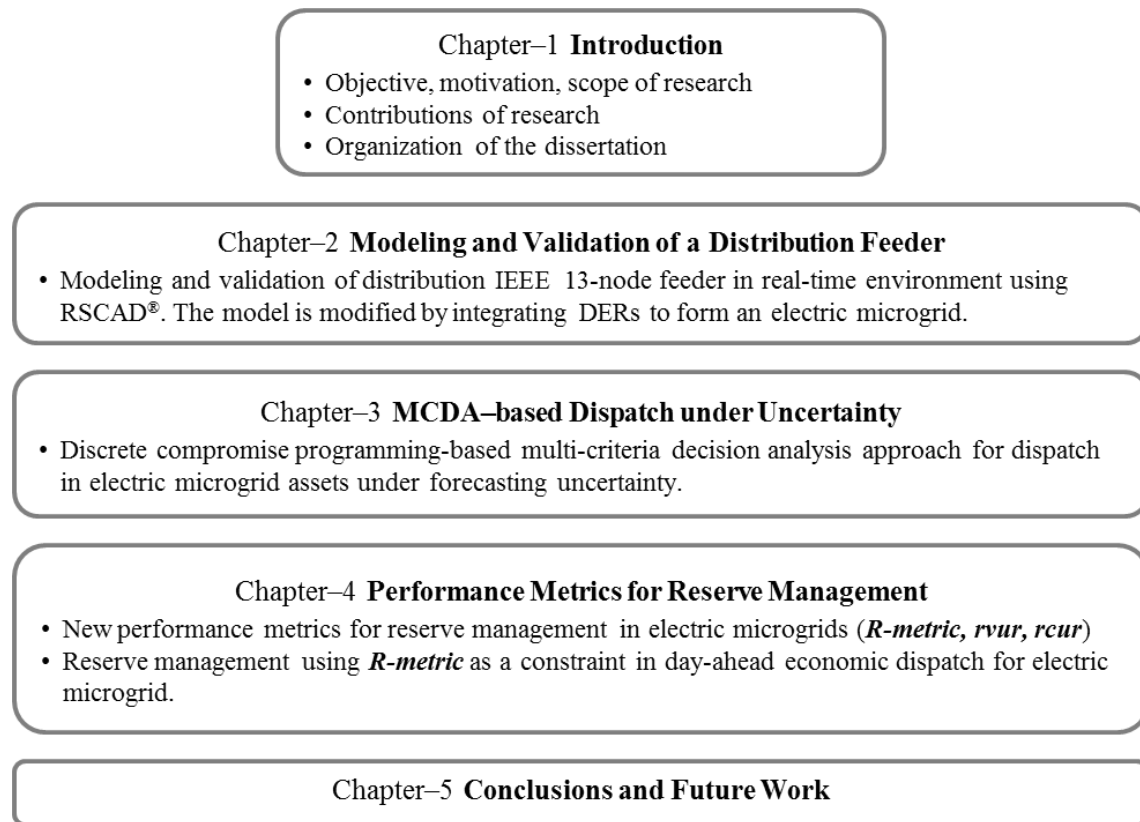


Figure 1.1 Organization of the dissertation with salient points of the work in each chapter

1.4 Tools and Techniques

RTDS[®] is used for modeling of power and control components, and real-time simulation. MATLAB[®] is used for realizing the optimization algorithm for multi-objective dispatch. MATLAB[®] is interfaced with RSCAD[®] script using Transmission Control Protocol (TCP)-based master/slave port-communication for sending dispatch set-points to the microgrid model. This simulates a centralized decision-making by distribution system operator (DSO) for day-ahead dispatch of the microgrid. Optimization in MATLAB[®] is done using goal attainment programming which is available as part of optimization toolbox. The decision-making using Discrete Compromise Programming (DCP) is scripted in MATLAB[®].

1.5 Additional research work

Some additional but related work was done as part of a contract with Idaho National Laboratory (INL) from 2014-2016. This additional research is related but does not coherently fit in the scope of this dissertation. Hence to maintain the coherency of the dissertation, only the closely related research is presented in this dissertation. A list of the publications from the additional work is presented in Table 1.2.

Table 1.2 Publications for additional research work as part of a contract with INL

Papers
1. M. Panwar , M. Mohanpurkar, J. D. Osorio, and R. Hovsopian, “Significance of dynamic and transient analysis in the design and operation of hybrid energy systems,” in <i>Proc. of the 9th International Topical Meeting on Nuclear Plant Instrumentation, Control, and Human Machine Interface Technologies</i> , 2015, p. 10.
2. Y. Luo, M. Panwar , M. Mohanpurkar, R. Hovsopian, “Real time optimal control of supercapacitor operation for frequency response,” <i>2016 IEEE Power and Energy Society General Meeting</i> , Boston, MA, 2016, pp. 1-5.
3. R. Liu, M. Mohanpurkar, M. Panwar , R. Hovsopian, A. Srivastava, and S. Suryanarayanan, “Geographically distributed real-time digital simulations using linear prediction,” <i>International Journal of Electrical Power & Energy Systems</i> , vol. 84, pp. 308–317, Jan. 2017.
4. J. D. Osorio, M. Panwar , R. Hovsopian, S. Suryanarayanan, J. Ordonez, “Multi-objective optimization of supercritical CO ₂ -based concentrated solar thermal power system operation,” under preparation.

Book chapter
1. M. Mohanpurkar, M. Panwar , S. Chanda, M. Stevic, R. Hovsopian, V. Gevorgian, S. Suryanarayanan, and A. Monti, “Distributed real-time simulations for electric power engineering,” in “ <i>Cyber-physical social systems and constructs in electric power engineering</i> ,” The Institution of Engineering and Technology (IET), London, UK, November 2016.

CHAPTER 2

MODELING AND VALIDATION OF A DISTRIBUTION FEEDER

1.1 Literature Review

A comprehensive literature review is presented on real-time simulation applications¹. The focus is on microgrids and related experimentation. An overview of distribution systems, real-time digital simulation environment, hardware-in-the-loop simulations with microgrid related applications, and modeling and validation results of distribution feeder in RSCAD[®] are presented in this chapter.

Electrical Distribution Systems

The electrical distribution system consists of low voltage to medium voltage electrical network (typically 34.5kV, 13.8 kV, 12.47 kV, 4.16 kV in US) [2.1], [2.2]. The distribution lines are short in length as compared to transmission lines and have comparatively higher R/X ratio, thus making line resistance non-ignorable in system analysis and operation. Typical distribution systems have non-transposed lines, unbalanced loads on different phases with different connections, two and single-phase lines, overhead and underground cables, distributed, spot, constant power (PQ), constant impedance (Z), and constant current (I) loads, voltage regulating devices [2.1].

Increased integration of synchronous and power electronic interfaced DERs requires detailed analysis using time-domain simulation tools. Electromagnetic Transient Program

¹Disclaimer: Chapter-2 is a verbatim reproduction of two peer-reviewed papers published in IEEE listed as Paper-1 and Paper-2 in Table 1.1 of Chapter-1 in this dissertation. The required permissions for re-use of the material have been obtained from the copyright holders and are included in the Appendix. The numbering of the figures and tables has been modified to satisfy the formatting requirements of the dissertation.

(EMTP)-based tools consider the electromagnetic interactions of various components in the grid and solve differential algebraic equations (DAE) at each time-step providing time-evolution of the system [2.3], [2.4]. This method is convenient to accurately capture high frequency phenomenon such as switching of power electronic converters in the system, with simulation time-steps in range of $50\mu\text{s}$ to $2\mu\text{s}$. Simulators such as Real Time Digital Simulator[®] (RTDS) use parallel processing using dedicated hardware to achieve real-time (RT) simulations with fixed time-step of $50\mu\text{s}$, and non-RT simulations at $2\mu\text{s}$ time-step [2.5]. RT simulations can be used with hardware-in the-loop (HIL) simulations without modeling the hardware component to be tested as a software model. An overview of RT HIL applications in microgrids, modeling and validation of distribution system in RTDS[®] are discussed in the following sections.

Real-time Digital Simulation Environment

Simulation tools for power systems can be classified as offline and real-time [2.6]. Generally, simulations are used for solving power network differential algebraic equations, planning, design testing, and deployment of a new system or post event analysis. Real time simulation tools have simulation time (and time steps) in synchronism with the real time as experienced by an actual wall clock. Transient network analyzers (TNA) using analog physical scaled down components have traditionally been used for real time simulation [2.7]. As the power system under consideration (simulation) became more complex with the integration of more distributed and renewable resources, the long set-up time, increased amount of effort required, and lack of reproducibility in designing physical analog models was no longer a practical option. Increases in computational power were also a driver for real time digital simulation. Thus, real time digital simulators were used for computationally intensive simulations where simulations took place in discrete time steps. The optimal power flow

solutions for digital computers were one of the primary steps in this direction [2.8]. Digital simulations used mathematical representation of systems through models of components, subsystems, and the associated dynamics instead of physical analog models [2.9]. This type of representation was convenient due to the ease of modeling using custom software, and the accuracy of the time response depended on the simulation time step, modeling granularity, and computation resource capabilities. More processors with distributed computation were used for software-based simulation, sometimes also called full-numerical mode of simulation [2.10]. Since, distributed computing requires partitioning of the system model on different processors for parallel computations; the decoupling is done using traditional state-space representation. However, such a technique may introduce high frequency poles and zeros close to the simulation sampling frequency. This type of error may be acceptable for slow dynamic transients in transmission networks with large time delays, but degrades the simulation accuracy for distribution networks with relatively shorter time delays. This can be solved without introducing artificial delays by using state space nodal (SSN) techniques [2.11]. Distribution systems are evolving from the traditional one directional passive power flow systems to active bi-directional power flow systems as a result of the integration of increasing numbers of renewable and distributed sources of energy. Distribution system studies employ different methods of analysis than transmission systems due to physical, electrical, and topological differences; a typical transmission network has a meshed structure, significant time delays associated with long line lengths, and a high X/R ratio to prevent electrical losses, while distribution systems have non-meshed topologies (in general), smaller cable lengths, shorter time delays, and higher ohmic losses due to lower X/R ratios. Transmission and distribution systems use different techniques for solving network equations and hence the need to address these differences in simulation also

arises. Digital simulators have been used for steady state, dynamic, and transient simulation and modeling. Switching power electronic devices can be included in simulation studies for long time-scale transient simulations without introducing much delay in the simulation; offline tools may give more accurate results, but the simulations take longer to compute. Real time digital simulations have been used to test various devices, components, controllers, protection schemes and configurations before launching a real world application.

The increasing penetration of power electronic interfaces in the distribution network requires high-resolution device modeling capabilities in digital simulation. Differences in design resolution requirements between distribution, transmission, and power electronics simulation have made it difficult to develop a simulation environment that captures the intricacies of all of the simulation types in the same platform. To address these issues, the digital simulator should be capable of fast and high time resolution simulations with faster convergence, should contain libraries and an editor for power electronic, semiconductor, control and firmware system modeling, and should be able to interface and communicate with other simulation platforms [2.12]. Some examples of real time digital simulations for power systems applications include: distributed computation for power systems [2.13], demonstration of a real time controller concept for distributed generation interconnection [2.14], a microgrid management system [2.15], a smart distribution grid laboratory [2.16], current relay testing and simulation [2.17], an active filter controller [2.18], interface protection and testing [2.19], STATCOM controller characterization [2.20], high-rated power electronics-based simulation [2.21], high temperature superconductor (HTS) motor testing [2.22], and small-signal analysis of wide area control system (WACS) [2.13], [2.23]. All of these application examples require detailed modeling for accurate digital simulation results. Since the real time response of digital simulation largely

depends on computation time and accuracy depends on modeling details, a combination of digital and analog models can be used to obtain high speed and accuracy. This technique employs external hardware to mimic a subsystem or a system component and multi-core processors to run portions of the simulation. Other challenges in the simulation of the evolving power system are to address the requirements of high-performance simulators, scalability, upgradability, and affordability.

Real-time digital simulation tools and HIL experimentation have been widely employed by researchers and practitioners for power system testing and analysis [2.6], [2.7], [2.9]-[2.22] . The complexity of evolving power systems has increased with the progressive integration of new technologies germane to the *Smart Grid*, distributed assets, and renewable energy sources. One such new addition to the existing electricity grid is the microgrid, which consists of a large number of small, heterogeneous assets interfacing to the electricity grid at the distribution level as a uniquely controllable entity. In order to de-risk the penetration of such new technology into a critical infrastructure like the electricity grid, it is imperative to attain full comprehension of the design and operation of the technological advancement. This requires a greater detail in system modeling and faster and more accurate simulation tools [2.11]. Though real time hardware-in-the-loop (RT-HIL) techniques have been extensively used for testing components, controllers, and protection devices and philosophies, applications related to microgrid operations remain not fully explored. The literature search performed here revealed several existing applications in distributed simulation of power systems, distributed resource integration, standard compliance testing, and interface protection testing [2.13], [2.14], [2.17]-[2.19]. However, there exist only a few applications related to microgrids [2.15], [2.16]. The existing applications have successfully and unequivocally demonstrated the use of RT-HIL in digital simulation for studies involving

isolated or stand-alone point assets and not so exhaustively for a microgrid. It is noted that this work does not claim preference of a particular platform of RT-HIL.

Hardware-In-the-Loop Simulations

HIL simulation involves interfacing hardware under test (HuT) to a simulated environment through HIL interfaces to a real-time simulation model [2.14], [2.24], [2.25]. This may take the form of controller HIL (CHIL) simulation, in which case the interfaces to the simulated system are through control level signals, with no significant power being transferred to or from the HuT. An example of CHIL simulation is illustrated by Figure 2.1, in which the power stage for some hardware is simulated along with a surrounding electrical system.

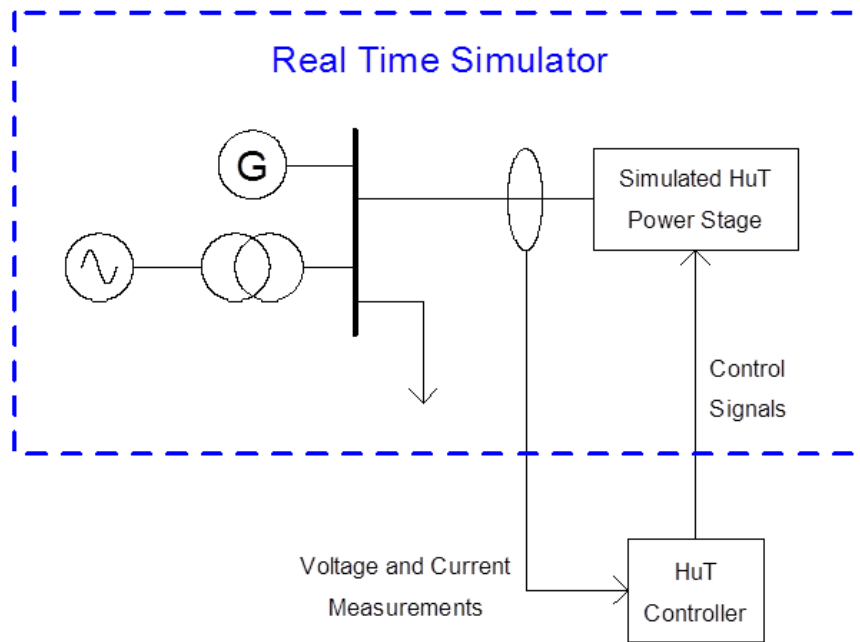


Figure 2.1 Example CHIL simulation

The controller HuT is interfaced to the simulated system through control level signals, using feedback of measured quantities in the simulated system (e.g., voltage, current, rotational speed), and providing control signals back to the simulated system (e.g., firing pulses, trip or reclose signals, reference quantities). This approach allows the HuT to be exercised in a realistic

environment such that system interactions and system integration issues can be studied and addressed. Because the surrounding system, and possibly power stage hardware for a developing technology, is simulated, these types of experiments can be conducted at the early stages (i.e., prototype) of a planned deployment of a technology. Additionally, because of the flexibility of the simulated system and the lack of risk for damaging equipment, this approach allows a wide range of scenarios to be explored, including extreme conditions which may be risky or difficult to reproduce with actual hardware. These types of experiments are also extremely valuable in collecting data for development and validation of models of the HuT, which can later be employed in other offline studies. Thus, CHIL simulation provides a flexible approach for testing of control systems, generally at considerably lower cost and risk than comparable tests conducted fully in hardware. As a distinction from CHIL simulation, power HIL (PHIL) simulation involves interfacing actual power hardware to a simulated system using power amplifiers and/or actuators (e.g., dynamometers). An example of PHIL simulation is illustrated by Figure 2.2, in which the HuT is interfaced to a simulated power system through a power amplifier.

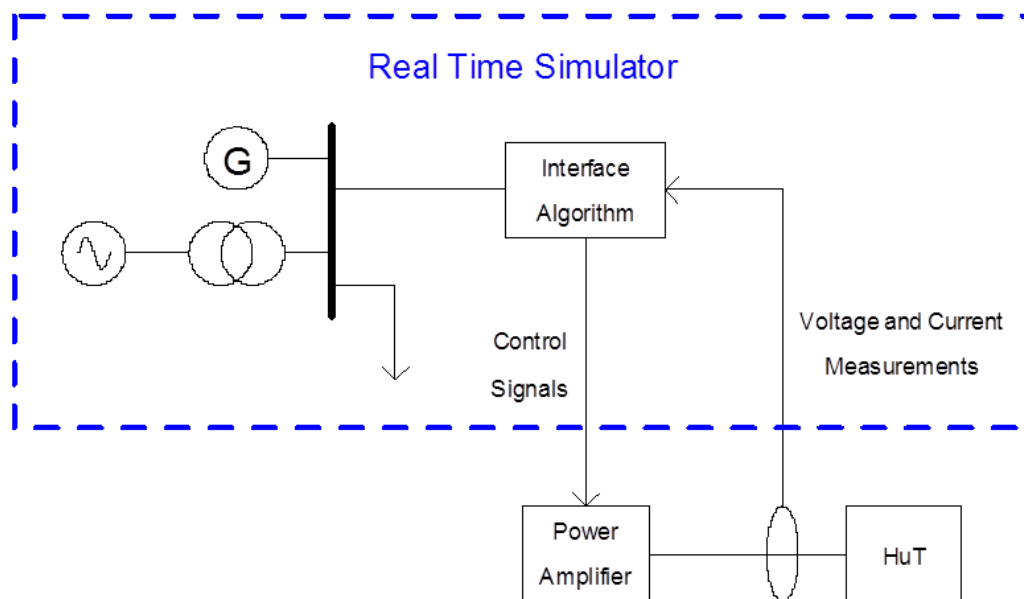


Figure 2.2 Example PHIL simulation

Interface algorithms implemented within the real-time simulation attempt to seamlessly couple the power hardware with the simulated environment. In this way, the HuT experiences the same stimuli and feedback that would be experienced in the actual system, and the simulation, in turn, experiences the effects of the HuT. This approach also affords substantial flexibility for varying the surroundings of the HuT and executing a wide range of scenarios, as compared to experiments conducted fully in hardware. Although the risk associated with PHIL experiments is increased compared with CHIL simulation, this approach also allows testing of extreme conditions within a controlled laboratory environment. Risk is posed to the HuT and the power amplifiers and actuators, but no risk is posed to the simulated equipment, and PHIL experiments can generally be more gracefully shut down if problems arise as compared to testing in the actual target system. Thus, this approach still facilitates a great deal of flexibility for exploring a range of surrounding systems and conditions, and obtaining experimental data for model development and validation. HIL simulation techniques are commonly used in the aerospace, automotive, and ship industries to evaluate new components, assemblies, and systems [2.22], [2.26], [2.27]. The use of HIL systems is also becoming popular for power electronics development [2.21]. Power electronics are considered as one of the enabling technologies for the emergence of the Smart Grid [2.28]. In particular, HIL applications for the grid integration and coordinated operation of renewable energy sources with energy storage [2.28], hybrid energy systems [2.29], advanced industry automation [2.30], and electric drive trains [2.31], [2.32] exist in the literature. The ability to design and automatically test power electronic systems with HIL simulation techniques reduces development cycles, increases efficiency, and improves reliability and safety of these systems for a large number of applications. This helps in designing, testing, validating, and optimizing the performance of an electrical system through real time simulations in a cost-

effective manner. Examples of accessing the performance of systems against established standards are presented in [2.14], [2.24], [2.33]. A demonstration that uses CHIL techniques, implemented in the RTDS real time simulator, to evaluate an application of an industrial controller based on IEEE Std. 1547 is presented in [2.14]. The work discusses the disconnection and reconnection of DG during and after faults as per the standard. The need of HIL for simulating this scenario arises from the fact that real time simulation for the distribution system over an extended period of time is required, which is not possible due to a lack of processing capability in non-real time simulators. Controller run-offs can be studied using RT-HIL to obtain actual response [2.34]. Hence, real time simulators with large data processing capability are suitable to capture and incorporate any system state change within the stipulated wait time of the DG before reconnection. However, data collection in RT-HIL simulation setups is a challenging task, which requires interfaces with additional assets such as DAQ systems [2.35]. Another CHIL example, presented in [2.18], utilizes a NI-PXI digital simulator containing the virtual power system model for testing a controller. Two tests were performed: one with a high switching frequency active compensator controller and a second with an overcurrent relay as the HuT. Reference [2.36] discusses the capabilities of HIL for specialized testing simulations in customer driven microgrids (CDM) where a commercial distributed control system (DCS) is the CHIL and real time digital simulator (RTDS) is used as the simulator. The configuration presented in [2.36] uses digital I/O interface amongst individual controllers in the DCS. Each controller can represent one power system component and a single microcontroller may represent a controller for multiple components. This addresses the issue of required scalability in testing the system as CDM becomes larger. Reference [2.38] describes the use of an OPAL-RT real time simulator for development of advanced inverter controllers. Some other applications of RT-HIL

such as superconducting fault current limiters [2.39], superconducting magnetic energy storage [2.24], power quality assessment [2.40], and large capacity photovoltaic array inverter testing [2.42] appear in the literature. The studies presented in [2.42] and [2.43] provide a detailed description of PHIL and interface issues concerned with stability of PHIL simulations. Since, PHIL consists of high power signals; inaccuracies in the simulations can damage the physical devices under test. The major errors can be attributed to limited convertor bandwidth, sensor noise, time delays and ripple in the interface amplifier. These issues are resolved by exploring various methods for stabilization and a new method is formulated with satisfactory performance. References [2.21], [2.44] present high power PHIL test beds and application examples related to 5 MW HTS motor testing, re-synchronization issues with DG, and power electronics controller tuning. An example of this configuration is the emulation of a PV array using a DC power supply [2.37]. Here the real-time system sends set point commands via the controller area network (CAN) protocol to the DC power source, which in turn measures its voltage and current output characteristics and sends them back to the real-time system. This PV array simulator is then used to perform a PHIL simulation by connecting the output terminals of the DC power source (in this case the power amplifier) to a PV inverter (or other DC load—the HuT), which then adds its dynamic response to the closed loop, full power simulation. These are some of the examples covering various possible applications of HIL for real time digital simulations. As noted in [2.45], while the HIL simulation paradigm offers an approach for thorough, early-stage testing of devices within realistic environments, several limitations and challenges with the approach must be recognized. The restrictions of real-time operation of the simulation model impose limitations on the size, complexity, and detail that can be captured by the models of the surrounding system. The HIL interfaces employed impose bandwidth limitations and introduce delays, distortion, and

noise which can affect the experiments and, in some cases, lead to instabilities. Additionally, the validity of the HIL experiments is limited by the validity and fidelity of the models used to represent the surrounding system.

Real-time Hardware-In-the-Loop Simulations for Microgrids

According to the IEEE Standard 1547.4-2011, an electric microgrid is defined as an electric power system (EPS) with the following characteristics: (a) contains distributed energy resources (DER) and loads; (b) contains local EPS or portions of the area EPS; (c) can disconnect to island or operate in parallel with area EPS; and, (d) islands intentionally [2.46]. Microgrids contain a heterogeneous mix of resources with asset capacity ranging from a hundred kW to a few MW. The participating assets can be DERs encompassing distributed generation (DG) – renewable and traditional generation and energy storage, or demand response (DR) type assets usually interconnected to the EPS at the distribution or sub-transmission levels [2.47]. Due to the small capacity ratings of the constituent assets, the number of such assets in a microgrid is much larger than the conventional EPS of a similar capacity. This may necessitate a need for newer control philosophies such as centralized co-operative control for the microgrid to handle the complexity of such a power system [2.15]. Microgrids differ from traditional power systems not only in terms of size and number of assets, but also in the nature of the assets. Heterogeneous power quality, security, and reliability issues can be addressed by microgrids [2.48]. Various configurations of DER, combined heat and power (CHP) assets, and photovoltaics (PV) in multi-MW microgrids have been explored in [2.49]. Finally, microgrids can offer reliable power to customers during duress, defer transmission and distribution capacity investments, increase energy savings, provide better power quality, reduce losses and environmental emissions, and also provide ancillary services such as frequency and voltage regulation, and reserves[2.50],

[2.51]. Several features of the microgrid scheme mentioned above make it a viable option for future advancements in power systems [2.51]. Standards are under development for the interconnection of DERs and their coordinated operation as part of a microgrid in grid-connected and islanded modes [2.46], [2.52]. Unlike in the transmission system, the line lengths associated with distribution systems are relatively small. Also, there is a high penetration of a considerably large number of fast switching power electronic interfaces for integrating renewable energy sources at the distribution level [2.11]. These characteristics are inherited by the assets in a microgrid. Hence, finer resolution of simulation times is required to capture transients as well as for the accurate modeling of pervasive power electronic devices.

To understand the actual response when components of a power system interact in a complex manner in a microgrid or finite inertia system, applications to realistic systems must be explored. Such a holistic view can be achieved with RT-HIL simulation applications in electric microgrids. While certainly distinguishing factors exist, microgrids share a number of common traits with shipboard integrated power systems (IPS). Reference [2.45] describes the potential role of HIL simulation in the development and deployment of new technologies for shipboard power systems. The qualitative pictorial representation of this potential role presented therein has been slightly adapted for more general applicability to power systems in Fig. 2.3. In Figure 2.3, time is represented on the horizontal axis, illustrating the stages of development and deployment of a new technology. The portion of the vertical axis occupied by each of the activities at any point in time is indicative of the relative effort associated with the respective effort at that point in time. It is anticipated that, in the early proof of concept stages, modeling and simulation would be heavily employed, with efforts quickly ramping into limited hardware testing. Even in these early stages, CHIL simulation may be used for development and testing of controllers.

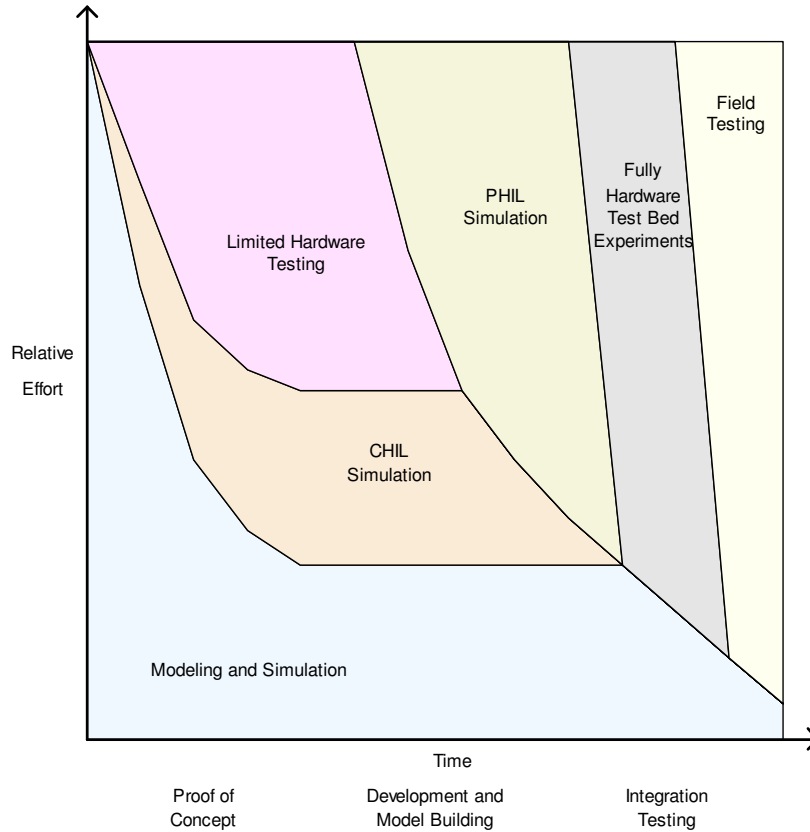


Figure 2.3 Potential role of HIL simulation

As development progresses, PHIL simulation may be employed for flexible testing of the device and collecting experimental data for model development and validation. CHIL simulation may facilitate early integration testing, as well as providing a means for de-risking of PHIL experiments through simulation of the PHIL setup. PHIL experiments may be used in proving the power hardware in realistic environments and addressing tests that may be riskier or more difficult to execute with fully hardware test beds. In the final stages, fully hardware test beds may be used to exercise and prove the hardware, without the constraints of bandwidth limitations, interfacing issues, and modeling assumptions. It is anticipated that the role of modeling and simulation will persist throughout the process, as models are used in preparation for experiments and are refined based on collected experimental data. In this view, HIL simulation is used to bridge the gap in integration testing between purely modeling and

simulation activities and the fully hardware test beds. Some of the challenges for real time simulation of microgrids are the same inherent problems as that of distribution systems and finite inertia power systems such as shipboard IPS. These include short cable lengths, large increased number of switching power electronic devices, and lack of flexibility and scalability. Due to the fact that the distribution cables have small time delay, it is not possible to partition the complex system for parallel processing. Any such attempt in real time simulation might develop algebraic loops, which can only be solved iteratively. This is not possible in real time simulations. State-space nodal solvers may be used to mitigate this issue [2.13]. Since the microgrid comprises of multiple systems with different simulation characteristics, the simulator must have a capability to run multi-resolution simulations. The issue of numerical stability arises with very small simulation time steps due to discretization of continuous time dynamics. This is addressed through use of SSN solvers. Reference [2.37] discusses and presents a test bed laboratory microgrid architecture consisting of wind turbine emulators, photovoltaic array emulator, micro-turbine based generation and load management system with controls for optimal asset dispatch. Similar cases can be extended to microgrids with analysis done for larger capacity and realistic systems using RT-HIL simulations. CHIL studies are expected to hasten to practice control and protection systems and methodologies that are germane to microgrid operations, especially ones with a mix of renewable and conventional generation. PHIL demonstrations are expected to accelerate the penetration of newer technologies such as those for energy storage within microgrids. The authors contend that the application of RT-HIL methodologies for characterizing the emerging microgrid concept will go a long way in its widespread penetration.

1.2 Modeling and Validation

The primary objective of this work is to describe some of the experiences and challenges faced in the development of models of an electric distribution feeder on a platform that supports HIL simulations. The platform of choice for the work presented here is RTDS-RSCAD, a real-time HIL environment, and the IEEE 13-node test system was chosen. The test feeder model did not exhaust the modeling capacity of one rack of RTDS, so this also provided the opportunity to extend this model to a DER integrated system. Other larger test feeders have more nodes to be modeled, which may require multiple racks of RTDS. This model captures the characteristics of a typical power system distribution feeder and can be validated against known results [2.56]. The IEEE-13 node distribution feeder is in the taxonomy of distribution feeder models provided mainly for testing power flow programs and other power system analyses using modeling and simulation. This feeder is highly unbalanced for a small 4.16 kV system, and consists of a mix of line phasing, overhead and underground lines, loads, capacitor banks, and a substation voltage regulator. A single-line diagram of the IEEE 13-node system is shown in Figure 2.4.

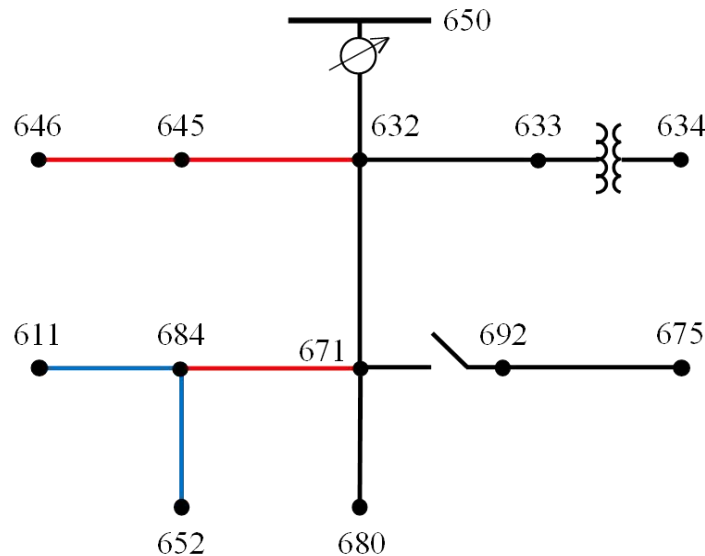


Figure 2.4 IEEE 13-node distribution test feeder

Three-phase, two-phase, and single-phase lines are denoted in black, red, and blue, respectively. RSCAD is the modeling interface and consists of a library of power and control system components. These library components were used to model the lines, loads, and controls for the test system. For the purpose of modeling the IEEE-13 node system, some of these models were modified to accommodate single-phase and unbalanced cases as discussed next.

Line Modeling

The lines in this test system are short—the maximum length of a line section is 2,000 ft, which restricts the options for using wave propagation type models for representing the distribution lines. Hence, PI-section models are used that require inputs for the R, L, and C values in the form of a matrix. Two to four phases can be modeled using the inbuilt PI model in RSCAD. Neutral is grounded, and the phase impedance and shunt admittance matrices are calculated offline using the data specified for the lines [2.1], [2.56], [2.58]. During the calculation of the shunt capacitance, the mutual capacitance values appear as negative. These are entered as absolute positive values in the PI-section model block as the internal calculations of the PI-section blocks assign negative signs to mutual capacitance values while formulating the admittance matrices. The three-phase and two-phase lines are modeled using this model block, while the single-phase lines are modeled using a PI-section model with R-L in series with C/2 in parallel at each end of the line.

Load Modeling

Three-phase and single-phase loads can be modeled in RSCAD using the built-in component models for three-phase and single-phase loads. The loads can be defined as constant power (PQ), constant impedance (Z), or constant current (I). As the inbuilt load block is defined as a dynamic load (i.e., PQ, Z, or I), the minimum, maximum, and initial values have to be

defined for each load type. The rating of the load is specified by the active and reactive power consumption at base voltage. This load rating is the control set point for the load. The set point can be provided either through some constant values in terms of real numbers directly in the load model, through sliders with initialized values and the option to change the variable during simulation in the Runtime environment, or by a 'ZIP' control block in RSCAD. This control block can be used to define what percent of the load is constant PQ, constant Z, or constant I. Such a control block is available only for three-phase loads. Three-phase loads can be either connected in Y or Δ configuration. As per convention of the IEEE-13 node test feeder system, the delta-connected load ratings for phase-A, phase-B, and phase-C refer to the ratings of the loads connected between phases A-B, B-C, and C-A, respectively [2.55]. The Y-connected load ratings are for each phase with the load connected between line and ground, and have the option of the common neutral to be grounded. If not specified, the neutral is grounded by default. The load is modeled as a dynamic component, and this characteristic is obtained by varying the conductance of the load. Three-phase loads can be modeled as balanced or unbalanced using the inbuilt three-phase dynamic load block in RSCAD. The load rating can be defined for each phase. The set point for a constant PQ load is independent of the node voltage. The set point for constant Z can be provided in the case of a balanced load but must be provided through sliders or constant real value. In the case of an unbalanced constant Z load or a constant I load, the P and Q values for the set point must be calculated offline and the values entered in the model block. Modeling blocks for single-phase dynamic loads are available in RSCAD, but the single-phase ZIP control blocks for providing P and Q set points to the load blocks are not available. Thus, it is convenient to model single-phase PQ loads where P and Q set points can be provided directly; however, a problem arises with constant Z and constant I loads, as no control blocks are

available for single-phase load set points. Single-phase constant Z loads can be modeled by calculating the real (R) and reactive (X) components of the load at bus voltage. Constant PQ loads are those that consume the same real and reactive power within a rated range of bus voltage variation that is defined by specifying minimum bus voltage in the load block. The control set points for constant-Z and constant-I loads are derived based the rated values of P and Q - P_{rated} and Q_{rated} , respectively [2.56]. The set points are dependent on the bus voltage V_{bus} (in pu) as given by (1). Single-phase controls for unbalanced and single-phase loads are built using control blocks in RSCAD using the relationships in (1), where α is 1 for a constant-I load, and 2 for constant-Z loads.

$$P_{setpoint} = P_{rated} \times V_{bus}^{\alpha}, Q_{setpoint} = Q_{rated} \times V_{bus}^{\alpha} \quad (1)$$

Line Drop Compensator

A compensator circuit is used to incorporate the voltage drop from the secondary side of the transformer for voltage regulator till the regulation node. The voltage and current are measured using potential transformers (PTs) and current transformers (CTs), respectively. The secondary side of the instrument transformer provides output at lower voltage and current levels, typically 120V for PTs and 5A for CTs [2.1], [2.55]. This method regulates the voltage at the secondary voltage regulator. Although the regulation node can be different from the secondary voltage regulator, the control circuit for the tap changer uses the compensated set point for control action, i.e., lowering or raising taps. The compensator R and X settings in volts are already provided in the IEEE-13 node test system. RTDS requires R and L values in ohms. The given values (in volts) are used for deriving the R (Ω) and X (Ω) ($L = X/2\pi f$, in H) values using the secondary current rating of the CT. The standard compensation circuit can be found in [2.1]. The relationship between the compensation circuit settings in volts and ohms is given in (2).

$$R + jX = \frac{R' + jX'}{CT_s} = \frac{(3 + j9)V}{5A} = 0.6 + j1.8 \Omega \quad (2)$$

The set point for the voltage regulator is derived based on the information presented in the IEEE-13 node document. The hold voltage value is 122V (on a 120V voltage base) with a bandwidth (BW) of 2V. This is used to compute the voltage regulation range set point $V_{RegSetPoint\ range}$ as shown in (3).

$$V_{Hold} - \frac{BW}{2} \leq V_{RegSetPoint\ range} \leq V_{Hold} + \frac{BW}{2} \quad (3)$$

A step change on the regulation transformer occurs only when the voltage feedback is outside this range. The feedback voltage at the secondary regulator is compensated with a voltage drop in the circuit until the regulation node. Thus, feedback voltage $V_{feedback}$ is given as shown in (4).

$$V_{feedback} = V_{RegulatorSecondary} - V_{Drop} \quad (4)$$

Voltage Regulator

The voltage regulator for the modeled test system is a three-phase wye connected transformer. Each phase is modeled using a single-phase grounded ideal transformer with the ratings specified for the test system. The turns ratio of the transformers is 1. The control circuit for the voltage regulator is built using control blocks in RSCAD and provides the set point for the step changes on the secondary voltage regulator. The controls for each phase are independent for individual-phase voltage control. The per-unit voltage of the regulation node was used for each phase and compared against a reference as permissible by the step change of the load tap changer and voltage control bandwidth. The node for voltage regulation is chosen by selecting the node with voltage less than 1 pu when there is no voltage regulation, no capacitors, and the

secondary side of the voltage regulator is at 1.05 pu [2.58]. The load tap changer in RSCAD is provided for three-phase transformers only. Thus, the tap changing logic was modeled based on information present in [2.57]. The LTC step size and range of operation is modeled as per the values in [2.55]. The LTC step size and range of operation is modeled as per the values in [2.55]. The leakage reactance, X_L , for the voltage-regulating transformer is not specified in the test feeder document. The default value in the RSCAD single-phase two-winding transformer is 0.04 pu, which is changed in steps of 1% in the range of 1%–7% to observe the effect on the voltage magnitude and phase angle errors. The plots of the magnitude and phase error profile versus X_L are shown in Figure 2.5.

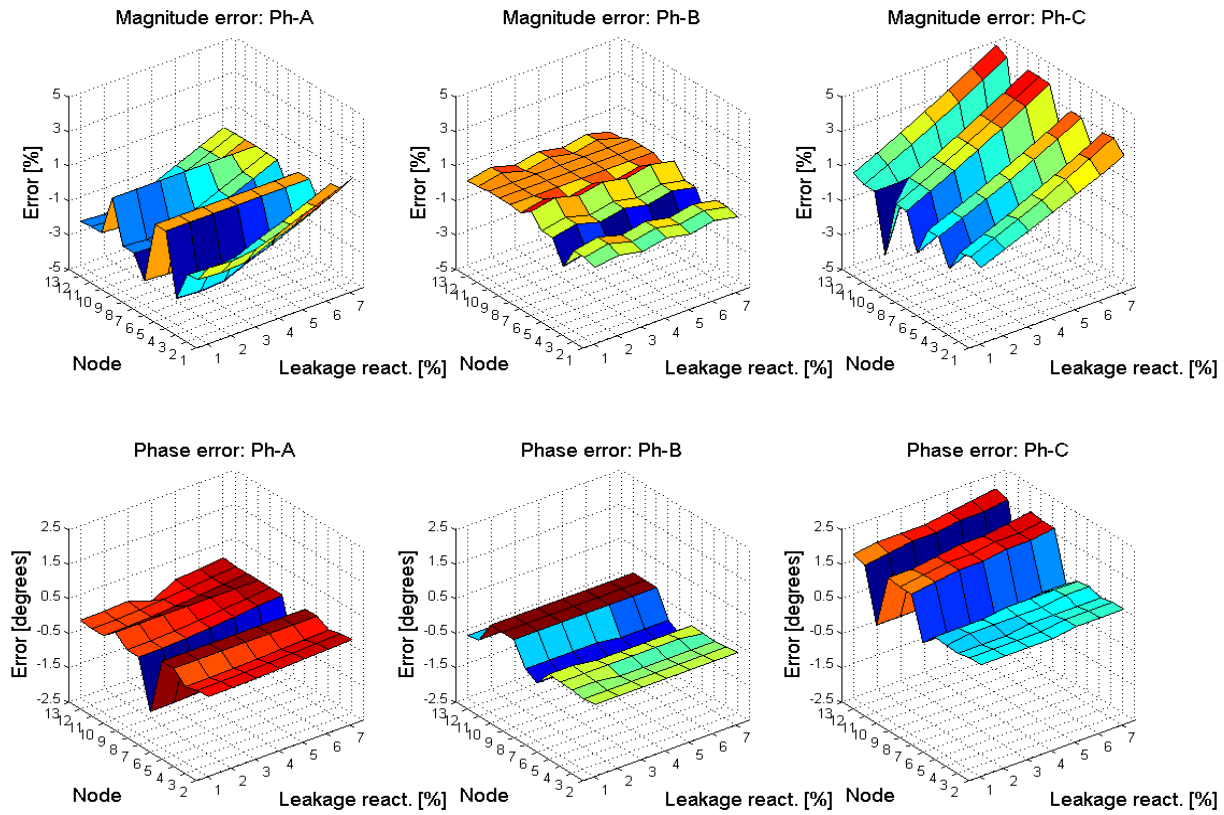


Figure 2.5 Error profile for voltage and phase angle with variation of the leakage reactance of voltage regulator transformers

Table 2.1 Error profile with variation of the leakage reactance of voltage regulator transformer

Error	Leakage reactance (%)	1	2	3	4	5	6	7
Voltage magnitude	Minimum	0	0.0281	0.1994	0.0284	0.1994	0	0.0303
	Maximum	3.6364	3.7374	3.6364	3.0303	3.0949	3.8737	4.6731
Phase angle	Minimum	0.1880	0.1810	0.1640	0.1390	0.1050	0.0410	0.0070
	Maximum	1.6670	1.7300	1.7300	1.7800	1.8300	1.9300	2.0300

Table 2.2 Steady-state voltage magnitude and relative error in %

Node		Phase - A		Phase - B		Phase - C	
		error		error		error	
VR	Measured	1.0625	-0.0471	1.0500	-0.3810	1.0687	1.0948
	Reference	1.0630		1.0540		1.0570	
632	Measured	1.0210	-1.0774	1.0420	-0.1919	1.0174	1.4154
	Reference	1.0320		1.0440		1.0030	
633	Measured	1.0180	-1.1788	1.0410	-0.1921	1.0148	1.3599
	Reference	1.0300		1.0430		1.0010	
634	Measured	0.9940	-2.9175	1.0218	-1.4876	0.9960	0.0703
	Reference	1.0230		1.0370		0.9953	
645	Measured			1.0329	-0.2033	1.0155	1.4279
	Reference			1.0350		1.0010	
646	Measured			1.0311	-0.1843	1.0134	1.4604
	Reference			1.0330		0.9986	
671	Measured	0.9900	-3.0303	1.0529	0.5604	0.9778	-0.0716
	Reference	1.0200		1.0470		0.9785	
680	Measured	0.9900	-1.8182	1.0529	0.0855	0.9778	2.0454
	Reference	1.0080		1.0520		0.9578	
684	Measured	0.9881	-1.8116			0.9758	2.0598
	Reference	1.0060				0.9557	
611	Measured					0.9738	2.0641
	Reference					0.9537	
652	Measured	0.9825	-1.7812				
	Reference	1.0000					
692	Measured	0.9900	-1.8182	1.0529	0.0855	0.9777	2.0354
	Reference	1.0080		1.0520		0.9578	
675	Measured	0.9835	-1.8810	1.0553	0.0284	0.9758	2.3468
	Reference	1.0020		1.0550		0.9529	

Table 2.3 Steady-state phase angle profile and absolute error in degrees

Node	Phase - A		Phase - B		Phase - C		
		error		error		error	
VR	Measured	0.00	1.13	-120.00	-0.41	120.00	0.36
	Reference	-1.13		-119.59		119.64	
632	Measured	-2.49	-0.14	-121.72	-0.42	117.83	0.73
	Reference	-2.35		-121.30		117.10	
633	Measured	-2.56	-0.18	-121.77	-0.47	117.82	0.72
	Reference	-2.39		-121.30		117.10	
634	Measured	-3.23	-0.28	-122.22	-0.52	117.34	0.74
	Reference	-2.95		-121.70		116.60	
645	Measured			-121.90	-0.4	117.86	0.76
	Reference			-121.50		117.10	
646	Measured			-121.98	-0.48	117.90	0.80
	Reference			-121.50		117.10	
671	Measured	-5.30	-1.59	-122.34	-0.84	116.02	0.42
	Reference	-3.71		-121.50		115.60	
680	Measured	-5.30	-0.20	-122.34	-0.64	116.02	1.72
	Reference	-5.10		-121.70		114.30	
684	Measured	-5.32	-0.20			115.92	1.72
	Reference	-5.12				114.20	
611	Measured					115.78	1.78
	Reference					114.00	
652	Measured	-5.25	-0.20				
	Reference	-5.05					
692	Measured	-5.31	-0.21	-122.34	-0.64	116.02	1.72
	Reference	-5.10		-121.70		114.30	
675	Measured	-5.56	-0.46	-122.52	-0.82	116.03	1.73
	Reference	-5.10		-121.70		114.30	

IEEE-13 node distribution test feeder has been modeled on the RTDS-RSCAD digital simulation environment and results verified with the standard results. The minimum steady-state voltage magnitude error is nearly 3% after voltage regulation using the LTC on the sub-station transformer. Challenges and experiences faced during the modeling are also discussed and solutions provided. This validated model is then used for integrating DERs and microgrid simulations.

REFERENCES FOR CHAPTER-2

- [2.1] W. H. Kersting. *Distribution System Modeling and Analysis*, 3rd Ed., CRC Press, 2012.
- [2.2] J. D. Glover, M. Sarma, T. Overbye, *Power System Analysis and Design*, 5th Edition, Cengage Learning, 2011.
- [2.3] H. W. Dommel, “Digital Computer Solution of Electromagnetic Transients in Single-and Multiphase Networks,” *IEEE Transactions on Power Apparatus and Systems*, vol. PAS-88, no. 4, pp. 388–399, Apr. 1969.
- [2.4] H. W. Dommel, “Techniques for analyzing electromagnetic transients,” *IEEE Computer Applications in Power*, vol. 10, no. 3, pp. 18–21, Jul. 1997.
- [2.5] Real Time Digital Simulator (RTDS), [Online]. Available: <https://www.rtds.com/>.
- [2.6] A. M. Gole, “Simulation tools for system transients: an introduction,” in Proc. *IEEE Power Engineering Society Summer Meeting*, 2000, v. 2, pp. 761–762.
- [2.7] O. Devaux, L. Levacher, O. Huet, An advanced and powerful real-time digital transient network analyser,” *IEEE Trans. Power Delivery*, v.13, no.2, 1998, pp.421–426.
- [2.8] H. W. Dommel, W. F. Tinney, “Optimal power flow solutions,” *IEEE Trans. Power Apparatus and Systems*, v. PAS-87, no. 10, 1968, pp. 1866–1876.
- [2.9] R. Kuffel, J. Giesbrecht, T. Maguire, et al., “RTDS-a fully digital power system simulator operating in real time,” in Proc. *Int’l Conf. on Energy Management and Power Delivery*, 1995, v. 2, pp. 498–503.
- [2.10] L. Snider, J. Bélanger, G. Nanjundaiah, “Today’s power system simulation challenge: High-performance, scalable, upgradable and affordable COTS-based real-time digital simulators,” in Proc. *Joint Int’l Conf. on Power Electronics, Drives and Energy Systems*, 2010, 10 pp.
- [2.11] R. Venugopal, W. Wang, J. Belanger, “Advances in real-time simulation for power distribution systems,” in Proc. *Int’l Conf. on Energy, Automation, and Signal (ICEAS)*, 2011, pp. 1–6.
- [2.12] J. Hambrick, S. Chakraborty, B. Kroposki, et al., “Current status of smart grid modeling and simulation,” White paper, National Renewable Energy Laboratory, Apr. 2010.
- [2.13] K. G. Ravikumar, N. N. Schulz, A. K. Srivastava, “Distributed simulation of power systems using real-time digital simulator,” in Proc. *Power Systems Conf. and Exposition*, 2009, pp. 1–6.

- [2.14] S. Suryanarayanan, W. Ren, M. Steurer, et al., "A real-time controller concept demonstration for distributed generation interconnection," in Proc. *IEEE Power Engineering Society General Meeting*, 2006, pp. 3.
- [2.15] J.-H. Jeon, J.-Y. Kim, S.-K. Kim, et al., "Development of HILS (hardware in-loop simulation) system for MMS (microgrid management system) by using RTDS," in Proc. *13th Power Electronics and Motion Control Conf.* 2008, pp. 2492–2497.
- [2.16] A. Yamane, W. Li, J. Belanger, et al., "A smart distribution grid laboratory," in Proc. *37th Annual Conf. on IEEE Industrial Electronics Society*, 2011, pp. 3708–3712.
- [2.17] A. Saran, S. K. Palla, A. K. Srivastava, et al., "Real time power system simulation using RTDS and NI PXI," in Proc. *40th North American Power Symp.*, 2008, pp. 1–6.
- [2.18] J. Wu, Y. Cheng, A. K. Srivastava, et al., "Hardware in the loop test for power system modeling and simulation," in Proc. *Power Systems Conf. and Exposition*, 2006, pp. 1892–1897.
- [2.19] M. Brenna, E. De Berardinis, L. Delli Carpini, et al., "Real time simulation of Smart Grids for interface protection test and analysis," in Proc. *14th Int'l Conf. on Harmonics and Quality of Power*, 2010, pp. 1–6.
- [2.20] L. Qi, J. Langston, M. Steurer, et al., "Implementation and validation of a five-level STATCOM Model in the RTDS small time-step environment," in Proc. *IEEE Power Energy Society General Meeting*, 2009, 6 pp.
- [2.21] M. Steurer, "PEBB based high-power hardware-in-loop simulation facility for electric power systems," in Proc. *IEEE Power Engineering Society General Meeting*, 2006, 2006, 3 pp.
- [2.22] M. Steurer, S. Woodruff, T. Baldwin, et al., "Hardware-in-the-loop investigation of rotor heating in a 5 MW HTS Propulsion Motor," *IEEE Trans. Applied Superconductivity*, v. 17, no. 2, 2007, pp. 1595–1598.
- [2.23] H.-M. Chou, K. L. Butler-Purry, "Real-time wide area power control studies using PXI and RTDS," in Proc. *44th North American Power Symp.*, 2012, 5 pp.
- [2.24] B. R. Lundstrom. "An advanced platform for development and evaluation of grid interconnection systems using hardware-in-the-loop," M.S. Thesis. Dept. of Electrical Engineering and Computer Science. Colorado School of Mines. May 2013.
- [2.25] J. Langston, M. Sloderbeck, M. Steurer, et al., "Role of hardware-in-the-loop simulation testing in transitioning new technology to the ship," in Proc. *IEEE Electric Ship Technologies Symp.*, Arlington, VA, Apr. 2013, 6 pp.
- [2.26] Z. Jiang, R. A. Dougal, R. Leonard, et al., "Hardware-in-the-loop testing of digital power controllers," in Proc. *21st IEEE Applied Power Electronics Conf. and Exposition*, 2006, pp.6.

- [2.27] J. de Jesus Lozoya-Santos, J. C. Tudon-Martinez, R. Morales-Menendez, et al., "Comparison of on-off control strategies for a semi-active automotive suspension using HiL," *IEEE Latin America Transactions, (Revista IEEE America Latina)*, v.10, no.5, 2012, pp.2045-2052.
- [2.28] W. Li, G. Joos, J. Belanger, "Real-time simulation of a wind turbine generator coupled with a battery supercapacitor energy storage system," *IEEE Trans. Industrial Electronics*, v. 57, no. 4, pp. 2010, 1137–1145.
- [2.29] L. Gauchia, J. Sanz, "A per-unit hardware-in-the-loop simulation of a fuel cell/battery hybrid energy system," *IEEE Trans. Industrial Electronics*, v. 57, no. 4, 2010, pp. 1186–1194.
- [2.30] S. Huang, K-K Tan, "Hardware-in-the-loop simulation for the development of an experimental linear drive," *IEEE Trans. Industrial Electronics*, v. 57, no. 4, 2010, pp. 1167–1174.
- [2.31] A-L. Allegre, A. Bouscayrol, J-N. Verhille, et al., "Reduced-scale-power hardware-in-the-loop simulation of an innovative subway," *IEEE Trans. Industrial Electronics*, v. 57, no. 4, 2010, pp. 1175–1185.
- [2.32] S. Grubic, B. Amlang, W. Schumacher, et al., "A high-performance electronic hardware-in-the-loop drive-load simulation using a linear inverter (LinVerter)," *IEEE Trans. Industrial Electronics*, v. 57, no. 4, 2010, pp. 1208–1216.
- [2.33] S. Suryanarayanan, M. Steurer, S. Woodruff, et al., "Research perspectives on high-fidelity modeling, simulation and hardware-in-the-loop for electric grid infrastructure hardening," in Proc. *IEEE Power Engineering Society General Meeting*, 2007, 4 pp.
- [2.34] J. Tang, Y. Gong, N. Schulz, et al., "Hardware Implementation of a ship-wide area differential protection scheme," in Proc. *IEEE Industrial and Commercial Power Systems Technical Conf.*, 2006, 7 pp.
- [2.35] J. Xu, S. Suryanarayanan, M. Steurer, "A controllable test bed to assess induction motor thermal behavior under time-varying voltage waveform distortions," in Proc. *39th North American Power Symp.*, 2007, pp. 136–142.
- [2.36] I. Leonard, T. Baldwin, M. Sloderbeck, "Accelerating the customer-driven microgrid through real-time digital simulation," presented at *IEEE Power Energy Society General Meeting*, 2009.
- [2.37] B. Lundstrom, S. Chakraborty, B. Kramer, et al., "An advanced platform for development and evaluation of photovoltaic inverters using hardware-in-the-loop," *Int'l Journal of Distributed Energy Resources and Smart Grids*, v. 9, Mar. 2013, PP. 25–44.
- [2.38] O. A. Mohammed, M. A. Nayeem, A. K. Kaviani, "A laboratory based microgrid and distributed generation infrastructure for studying connectivity issues to operational power systems," in Proc. *IEEE Power and Energy Society General Meeting*, 2010, 6 pp.

- [2.39] J. Langston, M. Steurer, S. Woodruff, et al., “A generic real-time computer simulation model for superconducting fault current limiters and its application in system protection studies,” *IEEE Trans. Applied Superconductivity*, v. 15, no. 2, 2005, pp. 2090–2093.
- [2.40] Y. Liu, M. Steurer, S. Woodruff, et al., “A novel power quality assessment using real time hardware-in-the-loop simulation,” in Proc. *11th Int’l Conf. on Harmonics and Quality of Power*, 2004, pp. 690–695.
- [2.41] J. Langston, K. Schoder, M. Steurer, et al., “Power hardware-in-the-loop testing of a 500 kW photovoltaic array inverter,” in Proc. *38th IEEE Industrial Electronics Society Annual Conf.*, 2012, pp. 4797–4802.
- [2.42] M. Dargahi, A. Ghosh, G. Ledwich, et al. “Studies in power hardware in the loop (PHIL) simulation using real-time digital simulator (RTDS),” in Proc. *IEEE Int’l Conf. on Power Electronics, Drives and Energy Systems*, 2012, 6 pp.
- [2.43] W. Ren. "Accuracy evaluation of power hardware in-the-loop (PHIL) simulation," Ph.D. Dissertation. Dept. of Electrical and Computer Engineering. The Florida State University. Dec. 2007.
- [2.44] M. Steurer, F. Bogdan, W. Ren, et al., “Controller and power hardware-in-loop methods for accelerating renewable energy integration,” in Proc. *IEEE Power Engineering Society General Meeting*, 2007, 4 pp.
- [2.45] J. Langston, M. Sloderbeck, M. Steurer, et al., "Role of hardware-in-the-loop simulation testing in transitioning new technology to the ship," in Proc. *IEEE Electric Ship Technologies Symp.*, Arlington, VA, Apr. 2013, 6 pp.
- [2.46] IEEE Guide for Design, Operation, and Integration of Distributed Resource Island Systems with Electric Power Systems, IEEE Std 1547.4-2011, 2011.
- [2.47] M. Panwar, G. P. Duggan, R. T. Griffin, et al., “Dispatch in microgrids: Lessons from the Fort Collins Renewable and Distributed Systems Integration demonstration project,” *The Electricity Journal*, v. 25, no. 8, 2012, pp. 71–83.
- [2.48] C. Marnay, “Microgrids and heterogeneous security, quality, reliability, and availability,” in Proc. *Power Conversion Conf. - Nagoya*, 2007, pp. 629–634.
- [2.49] R. H. Lasseter, “Smart distribution: Coupled microgrids,” *Proceedings of the IEEE*, v. 99, no. 6, 2011, pp. 1074 –1082.
- [2.50] S. Suryanarayanan, F. Mancilla-David, J. Mitra, et al., “Achieving the Smart Grid through customer-driven microgrids supported by energy storage,” in Proc. *IEEE Int’l Conf. on Industrial Technology*, 2010, pp. 884 –890.
- [2.51] M. Smith, “Overview of USDOE R&D activities on microgrid technologies,” presented at the *2009 San Diego Symp. on Microgrids*, San Diego, Sep 2009.

- [2.52] “WG C6.22 Microgrids - CIGRE.” [Online]. Available: <http://c6.cigre.org/WG-Area/WG-C6.22-Microgrids>.
- [2.53] M. Steurer, S. Woodruff, T. Baldwin, et al., “Hardware-in-the-loop investigation of rotor heating in a 5 MW HTS Propulsion Motor,” *IEEE Trans. Applied Superconductivity*, v. 17, no. 2, 2007, pp. 1595–1598.
- [2.54] National Instruments. Hardware-in-the-Loop (HIL) Test System Architectures. [Online]. Available: <http://www.ni.com/white-paper/10343/en>.
- [2.55] IEEE Power and Energy Society (PES). Distribution test feeders. [Online], Available: <http://www.ewh.ieee.org/soc/pes/dsacom/testfeeders/index.html>.
- [2.56] S. Suryanarayanan and R.G. Farmer, “Load modeling for stability studies,” Arizona State University. Tempe, AZ, Dec 2002.
- [2.57] H. Ravindra, “Dynamic interactions between photovoltaic inverters and distribution voltage regulation devices,” M.S. Thesis, Dept. of Electrical and Computer Engineering, Florida State University, Tallahassee, 2013.
- [2.58] W. H. Kersting, "Distribution feeder voltage regulation control," *IEEE Transactions on Industry Applications*, vol. 46, no. 2, pp. 620–626, Apr. 2010.

CHAPTER 3

DISPATCH OF MICROGRID ASSETS UNDER UNCERTAINTY

Introduction

Dispatch is a fundamental problem in electric power engineering that has been solved as a constrained optimization problem using various direct and heuristic techniques [3.1]-[3.8]². Traditionally, objectives such as operation cost, emissions, loss reduction, physical security and reliability along with physical limits of the power system as constraints are considered [3.1]-[3.5]. The increasing interest and progress in the development of the electric microgrid concept through demonstration projects, deployment, and testing indicates a few fundamental differences from the traditional electric power system (EPS) [3.7]-[3.11]. According to some well accepted definitions of an electric microgrid, the salient points that differentiate a microgrid from EPS are: local generation in the form of renewable and distributed energy resources (DER); demand response (DR); the ability to operate in grid-paralleled and islanded modes; and, the appearance to the EPS as a single controllable entity [3.12]-[3.18]. Other differences are based on the functions that the microgrid performs in context of the grid-connected or islanded modes of operation. A microgrid can be designed and used to serve various purposes such as reducing the peak load and losses in distribution grids, powering critical loads, enhancing reliability, reducing emissions through the deployment of renewables, maximizing profits from selling energy and ancillary services, and maintaining or improving power quality [3.16]-[3.19]. Thus, dispatch in microgrids can be posed as a constrained multi-objective optimization problem that can seek a

²Disclaimer: Chapter-3, in parts, is a verbatim reproduction of a paper under review with a peer-reviewed publication listed as Paper-3 in Table 1.1 of Chapter-1 in this dissertation. At the time of the preparation of this dissertation, the paper is under review. The numbering of the figures and tables has been modified to satisfy the formatting requirements of the dissertation.

near-optimum solution for a subset of objectives from the abovementioned list [3.18], [3.20]-[3.23]. Moreover, the preference of the objectives might not be available before the solution alternatives are obtained, and can also vary over the horizon of the dispatch. The variability and uncertainty due to the prediction errors of renewables makes the dispatch challenging. The uncertainty is handled through statistical distributions in [3.24]-[3.26] to identify intra-hour ramping/balancing needs in wind and solar integrated power system under California ISO. Stochastic scheduling is adopted with scenario-based approach in [3.27], and scenarios are used for day-ahead bidding for microgrids using hybrid stochastic/robust optimization in [3.28]. Scenario-based approaches can be computationally expensive and appropriate scenario reduction must be employed, as used in [3.29]-[3.31] for electricity markets, decision-making for planning and optimization. A state-of-the-art review of such techniques can be found in [3.32]. In [3.33]-[3.35], real time energy management in microgrids is presented with energy storage, and renewable uncertainties for finite-time horizon. The abovementioned applications and methods explore uncertainties with either single or aggregated objectives. In this work, we present the application of decision-making while considering multiple criteria through scenario-based finite-time horizon day-ahead dispatch. Due to the differences mentioned above and variety in functionalities, the dispatch in electric microgrids typically considers multiple objectives and therefore is more challenging than the dispatch in traditional EPS.

In this paper, a multi-criteria decision analysis (MCDA) based approach is presented for scheduling the dispatch in microgrids. Goal attainment programming is used to solve the multi-objective dispatch functional and discrete compromise programming (DCP) is applied as the MCDA technique for ranking the dispatch alternatives each hour for the decision maker (DM). DCP-based MCDA is a reference point technique where the best achievable value for each

objective is used as reference for decision making. DCP does not require a Pareto front to be generated for tradeoff amongst multiple objectives, and non-dominated solutions can be selected using L^p norms [3.36]-[3.37]. The rest of the chapter presents the formulation of the dispatch problem, goal attainment programming, DCP, and decision support system (DSS), the simulation setup and relevant input data, results and conclusions.

1.3 Day-ahead Dispatch under Uncertainty

Apart from the reasons mentioned in the previous section, the dispatch in microgrids is also challenging due to difference in contribution to the objectives to be met. The inherent characteristics of the dispatchable and non-dispatchable DERs might affect the objectives differently, at different times of the day. External factors such as policies, restrictions, controllability of DERs due to ownership, markets, and requirements of the DSO can also be crucial. To effectively dispatch the DERs to meet the objectives, these intrinsic heterogeneities and external factors must be considered in the dispatch methodology. Since the external factors are system specific and can vary with the domain of utility control, we focus on the intrinsic features of DERs. The uncertainty in output of DERs due to variability and forecasting errors are included in the day-ahead dispatch. In this regard, a multi-objective day-ahead dispatch methodology is presented by considering the influence of the DERs on the dispatch objectives. It is assumed that the DSO is the DM and has complete controllability of the dispatchable DERs. However, the DM does not have the perfect knowledge of the preference of the objectives due to the interdependence and conflict of different objectives, and hence an interactive support system for decision making is presented in the form of MCDA.

Problem formulation

The day-ahead hourly dispatch is formulated as a multi-objective problem with three objectives: minimization of operation cost, peak load, and emissions. These three objectives are some of the most highly preferred functionalities of microgrids and have been used in several microgrid projects worldwide [3.9]-[3.15]. More objectives can be considered without loss of general applicability of the techniques presented in this work.

Objectives

The first objective for the dispatch is the cost of operation. It is calculated based on Time-of-Use (ToU) pricing of electricity from the bulk EPS, and cost of fuel expended to generate electricity using the DERs present in the microgrid. Renewable energy sources such as solar and wind are assumed to have zero fuel cost of operation. The cost function for the optimization problem is shown in (1).

$$\varphi_1 = c_e p_e + \mathbf{c}_\mu^T \mathbf{p}_\mu \quad (1)$$

where, c_e , \mathbf{c}_μ are the costs of generation in \$/kWh and p_e , \mathbf{p}_μ are the generation outputs in kWh. The subscripts e and μ denote EPS and microgrid respectively, and the bold faced variable names denote vectors of length equal to the number of DERs in the microgrid. The microgrid considered here consists of a diesel generator, a solar photovoltaic (PV), and an electrical battery energy storage system (ESS) as DERs. The ESS is modeled as aggregated storage at the same node as PV. This can also be generalized as a community level ESS for aggregated residential rooftop solar [3.38]. The cost functions for EPS is the ToU pricing for electricity in Fort Collins, CO. The rate is based on Fort Collins Utilities' (FCU) 'ToU Rates Pilot Study' for residential customers during a summer weekday, and is given by (2) [3.39]. The on-peak hours are from

2pm to 7pm and all other hours are considered off-peak hours. The microgrid diesel generator quadratic cost function is given by (3) [3.40].

$$c_e = \begin{cases} 0.0670 \text{ \$/kWh}, & 1 \leq t \leq 13, 20 \leq t \leq 24 \\ 0.2249 \text{ \$/kWh}, & 14 \leq t \leq 19 \end{cases} \quad (2)$$

$$c_d = F_{max} \cdot f_d \cdot C_d \quad (3)$$

where $F_{max} = 42.8$ gal/h is the rated fuel usage of diesel generator in gal/h, $f_d = \alpha_2 \phi^2 + \alpha_1 \phi + \alpha_0$ is the fuel use rate, C_d is the cost of diesel in \$/gal, ϕ is the loading factor of generator in per unit, t is the time block in hours, and $\alpha_0 = 0.1524$, $\alpha_1 = 0.5780$, and $\alpha_2 = 0.2697$ are coefficients for diesel cost function in (3) [3.40].

The second objective is the load reduction during on-peak hours. The dispatch algorithm also allows the load reduction during the off-peak and on-peak hours. This objective is evaluated using the formula given in (4).

$$\varphi_2 = \frac{\sum p_\mu}{p_e + \sum p_\mu} \times 100\% \quad (4)$$

The third objective is the reduction of emissions due to fossil fuel used for power generation. The CO₂ equivalents for traditional EPS generators and diesel generators are considered. Carbon emissions due to renewable sources and energy storage are considered zero. The emission factor multipliers and the objective function equation are given in (5).

$$\varphi_3 = \chi_e p_e + \chi_\mu^T f_\mu \quad (5)$$

where $\chi_e = 1.800$ is emission factor for EPS [3.41], $\chi_\mu = [\chi_d; \chi_{pv}; \chi_{ess}]$ is the vector of emission factors for microgrid consisting of diesel ($\chi_d = 22.38$ lbs/gal), solar PV ($\chi_{pv} = 0$) and ESS ($\chi_{ess} = 0$), $f_\mu = [f_d; f_{pv}; f_{ess}]$ is vector of fuel usage for diesel, solar PV, and ESS [3.42], [3.43]. The values for emission factors are the upper limits on CO₂ emissions as per Environmental

Protection Agency (EPA), and the diesel and EPS generation are assumed to operate at these limits without violations.

Constraints

The constraints for the optimization procedure are the physical capacity limits of DERs, the load demand and generation balance, ramp rates for the diesel generation, and physical voltage constraints. These constraints are coded in the dispatch algorithm but ramping constraints become inactive for hourly dispatch since the ramp rates are very fast (several seconds to a few minutes from standby to full load) for the diesel generator in the microgrid. Energy storage is constrained to lower and upper limits of state-of-charge (SOC) requirements. Cycling efficiency of ESS is also considered. These are shown as in (6a-g).

Multi-objective dispatch using Goal Attainment

Goal attainment programming is used for solving the multi-objective dispatch problem. The objective functions considered in this work are not homogeneous in terms of physical units; further, they are also governed by different factors such as dispatchability, cost of fuel for operation, time period of the day, emissions. There are several other techniques for solving multi-objective problems including aggregation based methods such as weighted-sum-of-objectives or weighting method, ϵ -constraint method, and metaheuristic techniques that have been used in traditional power system and microgrid dispatch. Metaheuristic techniques such as genetic algorithms, simulated annealing, and tabu search are computationally intense but do not require the objectives to be convex. The ϵ -constraint method requires the DM to choose a single objective as the most preferred one, and the remaining objectives become constraints for the problem. This may become computationally cumbersome in the case of multiple runs, when a different objective is chosen as most preferred objective in each run. For non-commensurable

multiple objectives, which is often the case in real world problems, the solutions may be biased due to a forced choice of single preferred objective over the others. Scalarization through weighting method is straightforward to implement, but the disadvantages of aggregation methods are that they: do not provide any information about the trade-offs in optimization process; cannot explore non-convexities; and, can be computationally expensive when seeking a set of non-dominated or Pareto solutions. The solutions are biased due to the chosen weights and the method requires convexity as a property of solution search space. Goal programming is very similar to the goal attainment method in that it minimizes the weighted sum of the objective slack variables which represents underachievement. But, this method also suffers the same disadvantages as that of the other aggregation methods. Goal attainment programming does not require the convexity of the problem to find efficient solutions. This approach provides flexibility in searching for solutions in concavities by adjusting the preference weights, and the goals or target values to be achieved by each objective [3.21], [3.44], [3.45]. This approach also provides a good insight into the trade-off amongst conflicting objectives. The procedure aims to minimize the scalar γ , called the attainment factor. γ can take any real value, and the magnitude indicates over or underattainment of the objective. The problem formulation in standard form is shown in (6). The tilde denotes functions with stochastic variables.

$$\text{minimize } \gamma \tag{6}$$

$$\text{s. t. } \tilde{\varphi} - \mathbf{w} \cdot \gamma \leq \vartheta \tag{6a}$$

$$\mathbf{A}^T \cdot \tilde{\mathbf{p}} = \tilde{\mathbf{b}} \tag{6b}$$

$$\underline{\underline{\Delta \mathbf{p}}} \leq \frac{\Delta \mathbf{p}}{\Delta t} \leq \overline{\overline{\Delta \mathbf{p}}} \tag{6c}$$

$$\underline{\underline{\mathbf{p}}} \leq \mathbf{p} \leq \overline{\overline{\mathbf{p}}} \tag{6d}$$

$$\underline{\underline{\mathbf{v}}} \leq \mathbf{v} \leq \overline{\overline{\mathbf{v}}} \tag{6e}$$

$$\underline{soc} \leq soc \leq \overline{soc} \quad (6f)$$

$$soc(t + 1) = soc(t) + x_c \cdot \eta_c \cdot p_{ess} - x_d / \eta_d \cdot p_{ess} \quad (6g)$$

$$x_c \cdot x_d = 0 \quad (6h)$$

where $\tilde{\boldsymbol{\varphi}} = [\tilde{\varphi}_1; \tilde{\varphi}_2; \tilde{\varphi}_3]$ is the objective vector, $\mathbf{p} = [p_e; \tilde{\mathbf{p}}_\mu]$, $\mathbf{w} = [w_1; w_2; w_3]$ and $\boldsymbol{\vartheta} = [\vartheta_1; \vartheta_2; \vartheta_3]$ are dispatch, weight, and goal vectors respectively; \mathbf{A} , \mathbf{b} are the system matrix and the right-hand side equality constraint vector, respectively; (6c) and (6d) represent ramping and capacity constraints for the generators, respectively; (6e) is the node voltage constraint for allowable limits given as $\underline{v} = 0.95$ p.u. and $\overline{v} = 1.05$ p.u., for normal steady state operation as per ANSI voltage standard C.84.1 [3.46], [3.47]. (6f) is the SOC upper and lower limits equal to 0.3 p.u. and 1.0 p.u., respectively [3.33]. (6g) is the SOC update for time $t + 1$ based on power output of ESS at time t . (6h) has x_c and x_d as binary variables and represents constraint to avoid simultaneous charging and discharging decision. The constraint (6e) is not considered during the optimization process; rather, it is checked after the optimization procedure as an offline processing step for selecting feasible solutions. In case of violation of (6e) after running power flow in RSCAD[®], the next ranked solution as per MCDA is chosen. The cost of ESS operation is zero and power output is discretized into 5 levels, i.e. p_{ess} can take values from $\{0, 0.5(soc - \underline{soc}), (soc - \underline{soc}), 0.5(\overline{soc} - soc), (\overline{soc} - soc)\}$ at each hour. So, ESS can charge or discharge either 50% or 100% of allowable power capacity. This is a heuristic introduced here to make the look-ahead dynamic programming computationally tractable. This enables a simpler implementation, and a similar approach has been followed in [3.33]. The initial $soc = 0.5$ at start of 1st hour.

MCDA using Discrete Compromise Programming

The choice of a single or a small set of solutions based on a preferred value of objective is a difficult task when several objectives and alternatives are involved. A systematic method of ranking the alternatives must be used to obtain a feasible solution closest to the choices of the DM. Several techniques such as PROMETHEE and ELECTRE family of methods, and AHP have been used in literature for ranking, analysis and decision making when multiple alternatives are involved [3.44]. DCP is used here for ranking the solutions as per the chosen norm from the desired objective preferences. This is a reference point technique which is easy to implement and provides a best compromise and non-dominated solution from the set of alternatives without the need to generate a Pareto front [3.37], [3.38]. The formula for DCP norm calculation is shown in (7).

$$L_i^p(\varphi_i, \omega_i) = \left\{ \sum_{i,j}^{v,m} \omega_i \cdot \left| \frac{\varphi_{best} - \varphi_{ij}}{\varphi_{best} - \varphi_{worst}} \right|^p \right\}^{1/p} \quad (7)$$

where v is the number of objectives values (criteria), m is the number of dispatch options (alternatives), p is the norm index, ω_i is the user preference for the i^{th} objective, φ_{ij} is the value of the i^{th} objective for the j^{th} dispatch option, and φ_{best} and φ_{worst} are best-achievable and worst-achievable values of the i^{th} objective among all m alternatives.

DCP provides norm-based ranking formulas for multiple alternatives. The highest ranking solution is the one with least norm value and hence can be chosen by the DM as the best compromise solution. It should be noted that weights used in the optimization process, \mathbf{w} is different from the weights $\boldsymbol{\omega}$ used in (7) for MCDA. There is no restriction on the values of $\boldsymbol{\omega}$ and can be chosen by the DM per the preference of objectives. At each hour, two-hour look-ahead scheme is implemented to find the evolution of the objective function values. This

provides $5^3 = 125$ alternatives to choose from and MCDA is used to rank these alternatives. Total sum of each objective function values over t , $t + 1$, and $t + 2$ are used as *cost-to-go* function.

Decision Support System for DSO

The multi-objective goal attainment programming is used to solve the day-ahead dispatch optimization problem at each time period. A dynamic programming routine is used for look-ahead dispatch considering the present and the next two hours. The ESS power output is chosen from 5 discrete levels and used as a fixed value in goal attainment program to solve the dispatch for the particular choice of ESS. This generates 125 possible alternatives, each with one set of objective function values. These alternatives are then used in the DCP-based MCDA process to obtain the most preferred option based on DCP preference weights ω provided by the DM. The DM can revise the preference weights ω , if the dispatch is to be revised. The provision of revising weights and seeking a more satisfactory alternative enhances the interactivity of DM in process of MCDA. The DM can choose the preference weights for each time period and the DCP provides the ranking of feasible alternatives based on closeness to the desired values, based on the DM preference. The top ranked solution is used to check the power flow constraints in RSCAD[®]. If the constraint violation occurs, the next rank solution is chosen. The weights depict the preference of the objectives. During a particular dispatch optimization routine, the weights are allowed to vary during a transition from off-peak to on-peak hours and vice-versa, to coincide with the ToU pricing methodology used in the study here. The weights remain fixed during all hours of the off-peak or the on-peak period. Fig. 3.1 shows the flowchart for the process. Dispatch optimization and simulations are performed for each scenario based on load and solar stochasticity.

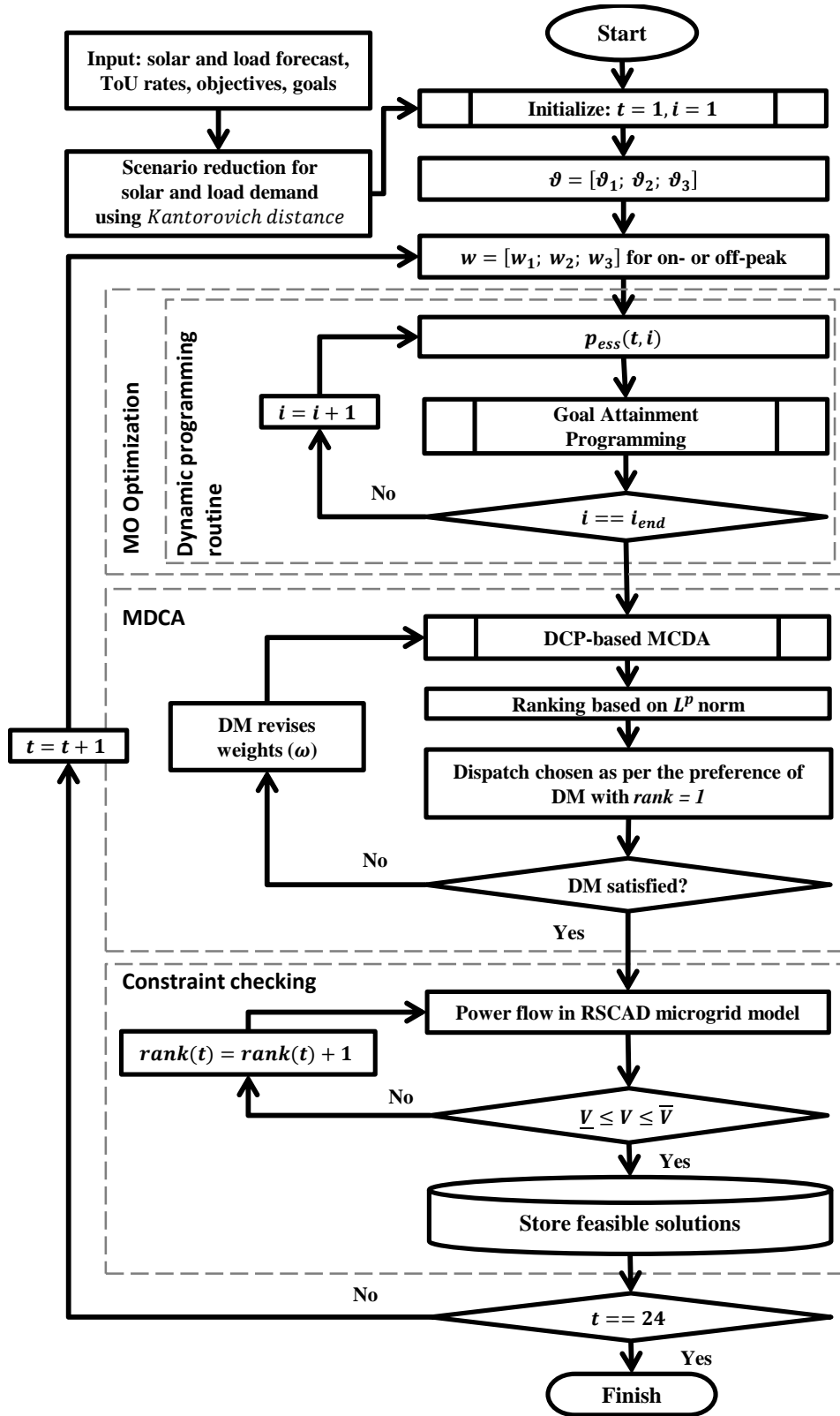


Fig. 3.1. Flowchart for dispatch using goal attainment and DCP-based MCDA.

Fig. 3.2 illustrates the DCP-based MCDA applied to a one-variable, two-objective optimization problem. The actual simulations considered three objectives and two optimization variables for dispatch but this simple case is chosen for clarity in visual representation and explanation of the process. The portion shaded in green is the decision space for two conflicting objectives φ_a , and φ_b . Each point in the decision space represents a set of feasible objective function values obtained from simulation by using different sets of preference weights for the objectives. The set of non-dominated solution at time t is represented by the compromise set S_t . A best compromise solution x_t is chosen based on the DCP-based MCDA without generating a Pareto front. This dispatch solution is used to decide the set of feasible solutions $FS_{t+1} = (S_{t+1}|x_t)$ for the next time-period $t + 1$. Dynamic programming routine for look-ahead dispatch optimization subsumes this feature by considering the SOC constraint of ESS in previous time-step.

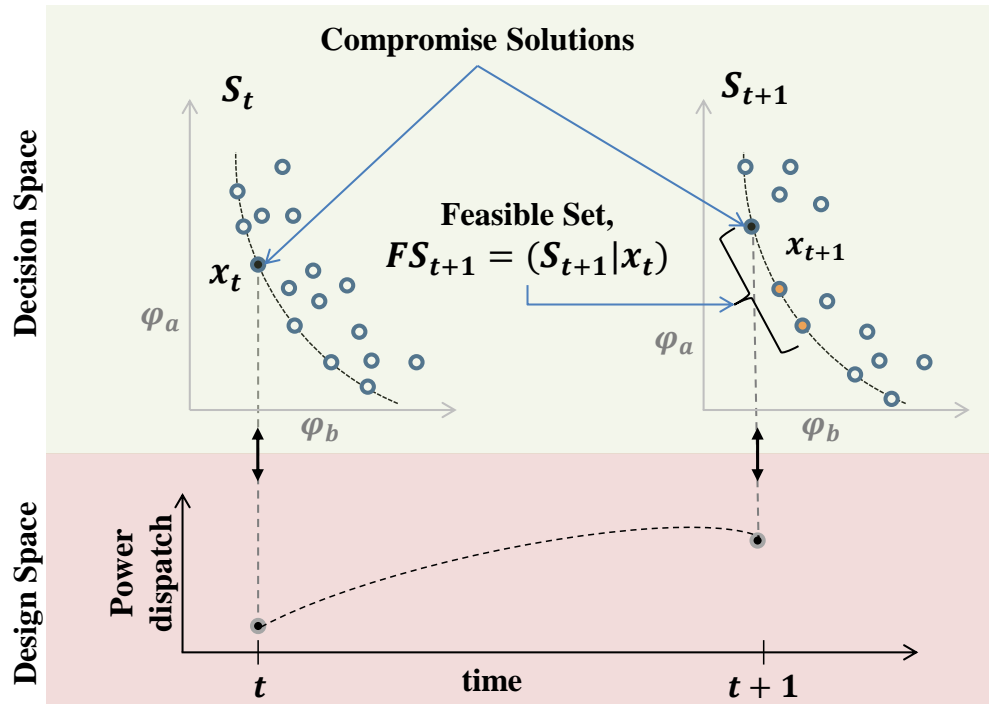


Fig. 3.2. Illustration of MCDA applied to set of solutions from the multi-objective optimization dispatch problem.

The selected solutions obtained using DCP-based MCDA is given below in (8a) and (8b).

$$x_t = DCP(S_t) \quad (8a)$$

$$x_{t+1} = DCP(FS_{t+1}) = DCP(S_{t+1}|x_t) \quad (8b)$$

Thus, it may be noted that the feasible sets of compromise solutions may change depending upon the choice of the preference weight sets by the DM for MCDA at each time period.

Simulation Setup

The dispatch optimization is done using MATLAB[®] and the interfacing is done with RunTime[®] of RSCAD[®] using a TCP server-client-based port communication. The set points from dispatch solutions are sent to the diesel generator model in RSCAD[®] along with the solar irradiance and air temperature to the solar PV model for each hour.

Microgrid Modeling

The microgrid is modeled by modifying the IEEE 13 node feeder [3.47]. The modification is done by integrating two DERs at nodes 634 and 680. The platform used for modeling is RSCAD[®]. The microgrid consists of a synchronous generator driven by a diesel engine [3.48], and a solar PV array with two-stage, two-level DC/AC power converter [3.49]-[3.52]. ESS is modeled as a three-phase controlled current injection for desired power set points. DER ratings are shown in Table 3.1.

Table 3.1 DER ratings and interfaces in the microgrid

DER	Rating	Interface
Synchronous generator	0.60 MVA, 0.48 kV	0.48 kV/0.48 kV, Δ -Y
PV VSC converter	0.35 MVA, 0.48 kV	0.48 kV/4.16 kV, Δ -Y
Energy storage	0.30 MVA, 4.16 kV	Controlled I -injection

A dynamic model is used for synchronous generator [3.53], and switching model is used for simulating the PV using the Voltage Source Converter (VSC) small-time step modeling in RTDS[®] [3.54]. The solar PV are rated at 350 kW, and the small-time step VSC converter is interfaced to large time-step model using three single-phase interfacing transformers. Fig. 3.3 shows the simulation setup. It may be noted that RSCAD[®] is used here as a preferred platform for modeling and simulations to tie the present work with some ongoing and future projects which require a platform such as RSCAD[®]. Any other steady state modeling and simulation platform can be used to verify voltage constraint violations.

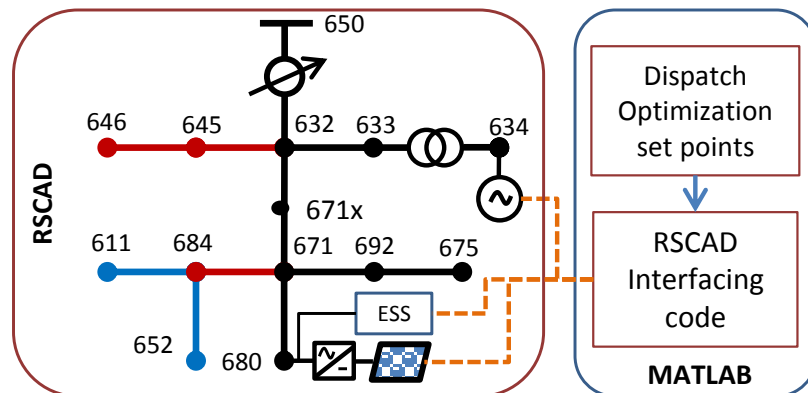


Fig. 3.3 Microgrid model using IEEE 13 node feeder and DERs in RSCAD[®] interfaced with dispatch optimization code in MATLAB[®].

Simulation data

The operation cost of the solar PV is assumed to be zero. The hourly data for solar irradiance and temperature are obtained for August 19, 2015 in Fort Collins, CO, USA [3.55]. The intra-hour solar irradiance data for 10 minute time intervals is used to obtain variation of solar irradiance during the hour. These variations are normally distributed about the hourly mean values, and are fit to a normal distribution [3.24]-[3.26]. The intra-hour variations data are fit for low ($\leq 600 \text{ W/m}^2$, 6am to 10am, and 4pm to 8pm) and high irradiance time intervals ($>600 \text{ W/m}^2$, 10am to 4pm). This is done to accurately account for low and high statistical variance during high and low irradiance periods respectively [3.26]. The diesel data is taken for the Rocky Mountain region from [3.56]. The cost for diesel generator is given by (3). The solar irradiance profile is shown in Fig. 3.4, and the model for the solar PV panel is given in (9) [3.8].

$$p_{pv} = p_{rated} \frac{S_{irr}}{S_{stm}} [1 + k(T_c - T_r)] \quad (9)$$

where S_{irr} is the solar irradiance in W/m^2 ; $S_{stm} = 1000 \text{ W/m}^2$; $k = -0.0046$; $T_c = 25^\circ\text{C}$, and T_r is temperature of solar array.

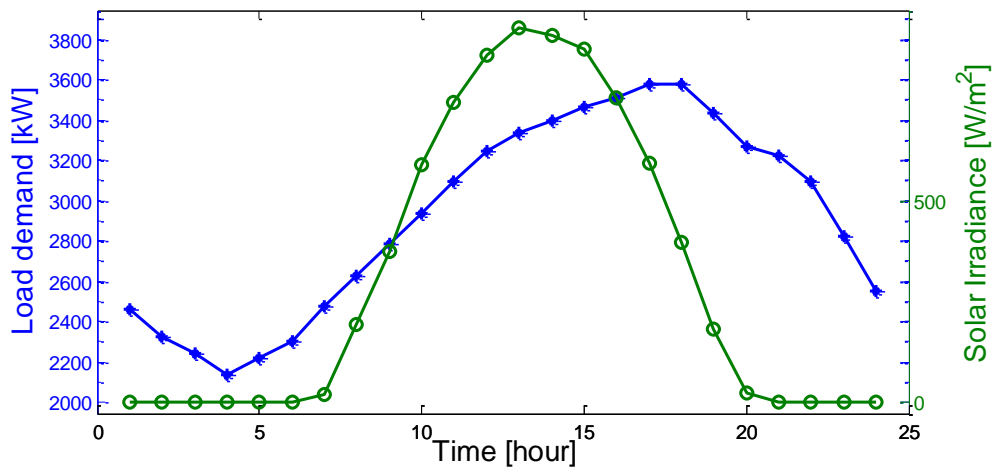


Fig. 3.4 Solar irradiance profile for Ft. Collins, CO and load demand profile used for simulation [3.55]. Load data is taken from PRPA [3.57] forecast and scaled down for the microgrid simulations [3.58]. Both data are for August 19, 2015.

The data for the load demand curve is obtained from Platte River Power Authority (PRPA) system forecast for August 19, 2015 [3.57] and scaled down linearly to IEEE 13-node feeder load of 3.577 MW [3.58]. The load demand is assumed to be normally distributed about the mean value equal to hourly forecast. Scenarios are generated to include the stochasticity of the solar irradiance error and load variation. The empirical distributions are sampled for $\mu_{load} \pm 1.5\sigma_{load}$ for load and $\mu_{solar} \pm 3\sigma_{solar}$ for solar irradiance to generate scenarios. Statistics are shown in Table 3.2 below.

Table 3.2 Empirical distribution statistics (μ, σ) for scenario generation

Irradiance/load demand	Solar error (W/m ²)	Load demand (p.u.)
High	(16.3778, 95.8512)	(0, 0.0434)
Low	(-11.2937, 157.7270)	(0, 0.1111)

Joint distribution is obtained and the cases with joint probability > 0.1 are considered. 5000 scenarios are selected using uniform random sampling from the above cases. Each scenario is a 24 hour profile consisting of a pair of load and solar irradiance profiles. Scenario reduction is done to avoid computational intractability and 5 representative scenarios are obtained using *Kantorovich distance* which uses *Wasserstein metric* of prescribed order r . We use $r = 2$ which is representative of pairwise Euclidean distance between two samples of the selected scenarios. This approach has been used in scenario reduction in power system simulations in [3.29]-[3.30], [3.32]. The distribution of the 5000 scenarios and 5 representative scenarios used in the simulations is shown in Fig. 3.5. It can be observed by visual inspection that both the original and reduced scenarios have similar distributions. Quantile-quantile plots are used to ensure

linearity between the original and reduced distributions as shown in Fig. 3.6. Emission data for the EPS and diesel generators are obtained from [3.42] and [3.41], [3.43], respectively.

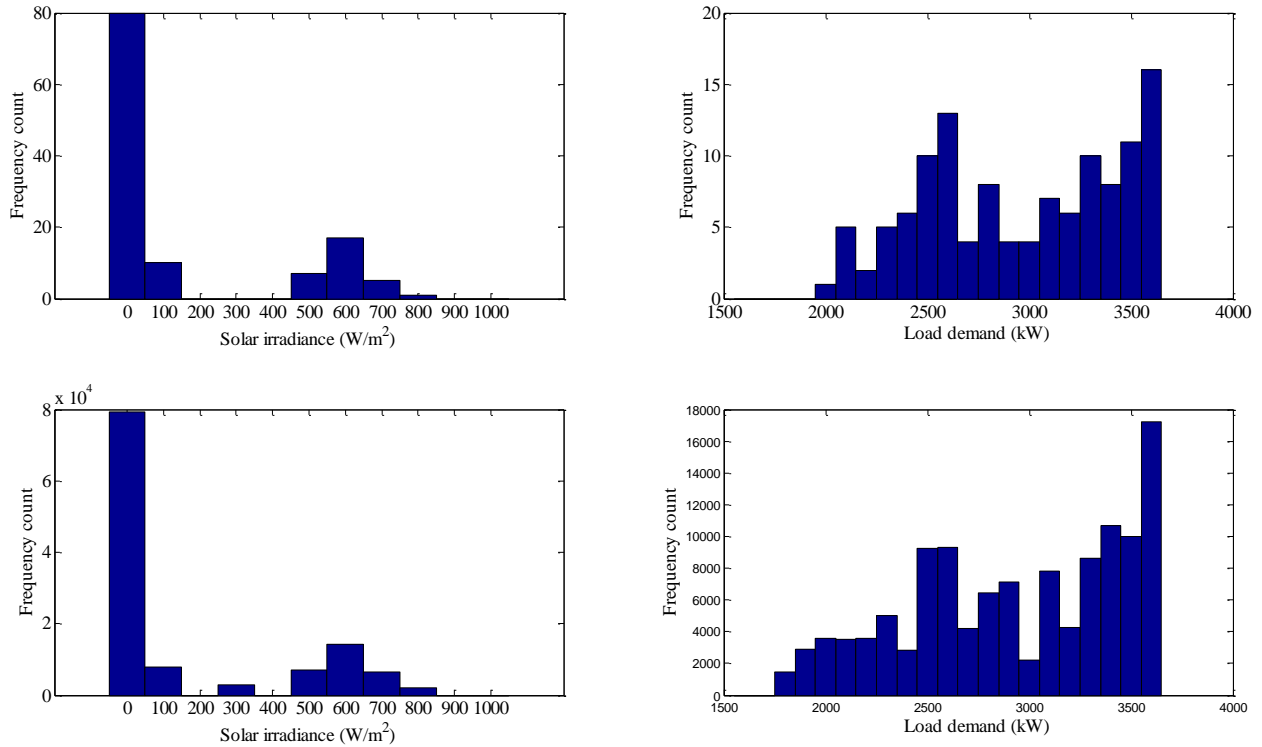


Fig. 3.5 Distributions of sampled scenarios for simulations (Top-left and bottom-left are the plots for reduced and original scenarios for solar irradiance, respectively; Top-right and bottom-right are the plots for reduced and original scenarios for load demand, respectively)

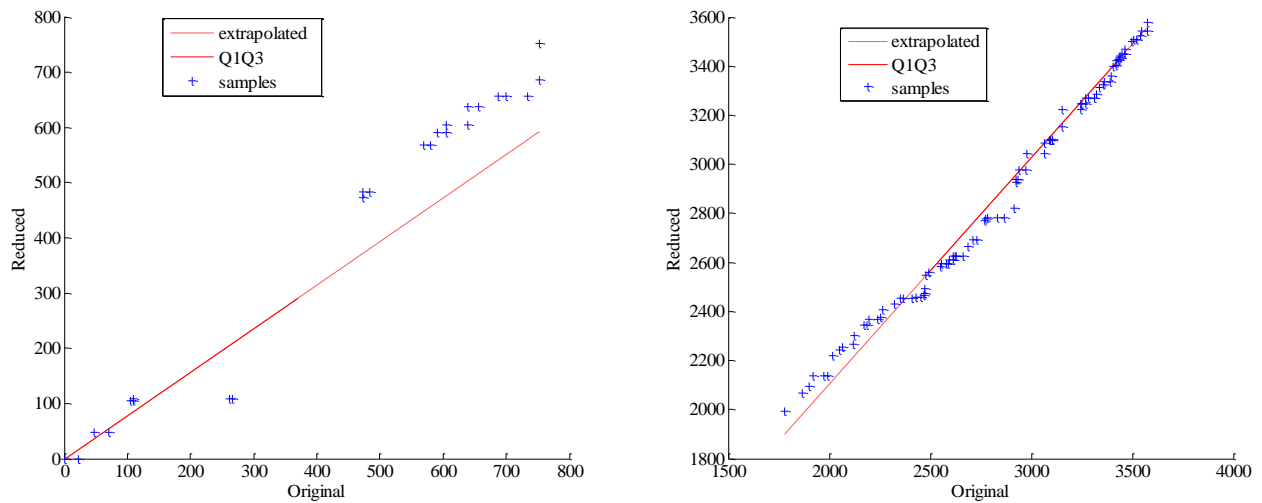


Fig. 3.6 Q-Q plots for the original and the reduced scenarios (Left: Load demand in kW; Right: Solar irradiance in W/m²)

The goals used for the optimization are based on the baseline values obtained from an EPS only case, i.e., when no DERs are present to serve the load and the electricity is served from EPS. These values are used to derive goals for dispatch optimization in presence of DERs. The target for the operation cost is set same as the EPS baseline case. The goal for peak load reduction is set based on time of the day, i.e., the percent peak load reduction (PLR) during on-peak and off-peak times is 20% and 0%, respectively. The goal for emission reduction is 70% of the baseline which is also in close accordance with Clean Air Act (CAA) [3.41]. The preference weights ω are chosen by the decision maker for each objective as 1, 10, or 100. A chosen set of weights remains constant for all hours in an on-peak or off-peak period, but variation between on-peak and off-peak are allowed. This is to reflect a change in preferences in objectives during the on-peak and off-peak hours.

3.2 Simulation Results

The example case simulated in RSCAD[®] considers a microgrid where the DSO has the following preference for the objectives, $\omega = [10, 100, 1]$ during on-peak hours and $\omega = [1, 1, 10]$ during off-peak hours. Such a case will represent a microgrid with the main functionality of peak shaving during on-peak hours. For purposes of scheduling, the diesel generator idling is avoided by starting the generator when needed instead of considering the contributions to cost and emissions without any contributing power output. The function outputs for 5 scenarios weighted by their respective probabilities are shown in Fig. 3.7. The operating cost and emissions are normalized by the goals at each hour. The values of operating cost and emissions equal to 1 p.u. depict exact attainment of goals, while less than or greater than 1 p.u. represent over- and under-achievement, respectively. The load reduction objective is also represented as a normalized value. The goal used for normalization is modified by adding 1.0 both in denominator and

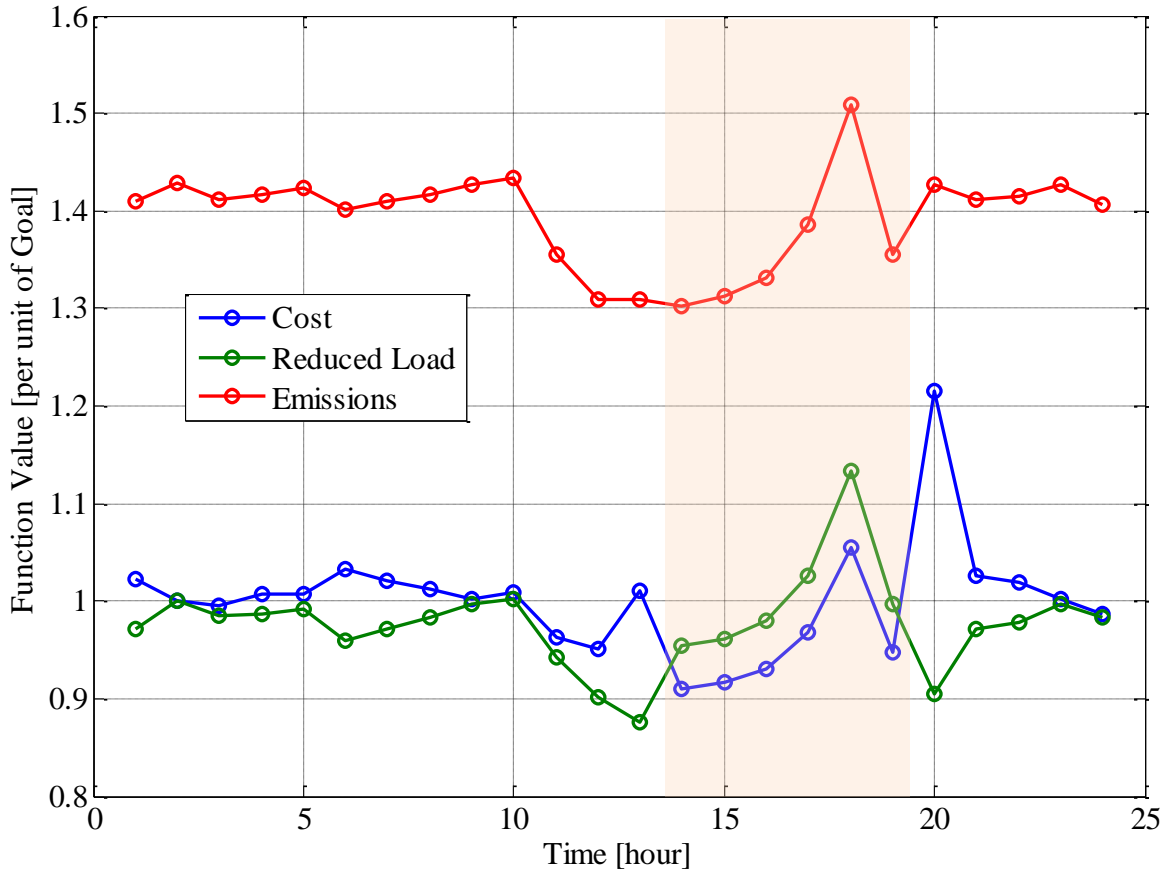


Fig. 3.7 Hourly objective function values for stochastic scenarios and preference weights $w = [10, 100, 1]$ during on-peak hours and $w = [1, 1, 10]$ during off-peak hours. MCDA preference weights are also set as $\omega = [10, 100, 1]$ and $\omega = [1, 1, 10]$ in this case. Shaded portion depicts on-peak hours.

numerator only for representation purposes to avoid divide by zero when PLR goal is 0%, such as the case during off-peak hours. This value represents load demand attained as per unit value of the target load demand after reduction, and is represented in p.u. The load reduction goal is 20% during peak hours which is achieved closely to the target during most hours except in 17th and 18th hours, where it is under-achieved by factors of 1.03 and 1.13. This is due to reduction in solar output in 17th hour, and charging of ESS in the 18th hour which discharges partially in the next hour to meet load reduction goals. Since the dispatch considers two hour look-ahead approach, the ESS makes a decision to charge during 17th hour and provide power during next

hour. This also makes sense intuitively, since the goals of load reduction is zero during off-peak hours. The look-ahead dispatch enables optimal decisions to be made for present time accounting for next two hours. The change in preference weights is also accounted for and optimal actions are taken considering finite time horizon. During off peak hours also, the attainment of objectives is close to the goals. The peak in the operating cost at 20th hour is due to one major factor governed by EPS ToU pricing. The goal in this case is equal to the base cost of operation of EPS. This value is used in denominator for normalization and is lower during off-peak hours. This influences the function value depicted as per unit of the goal. The rise of this value during 18th hour is because solar output is zero, the diesel generator is operating at maximum, and EPS import increases to charge the battery for achieving load reduction as shown in Fig. 3.8.

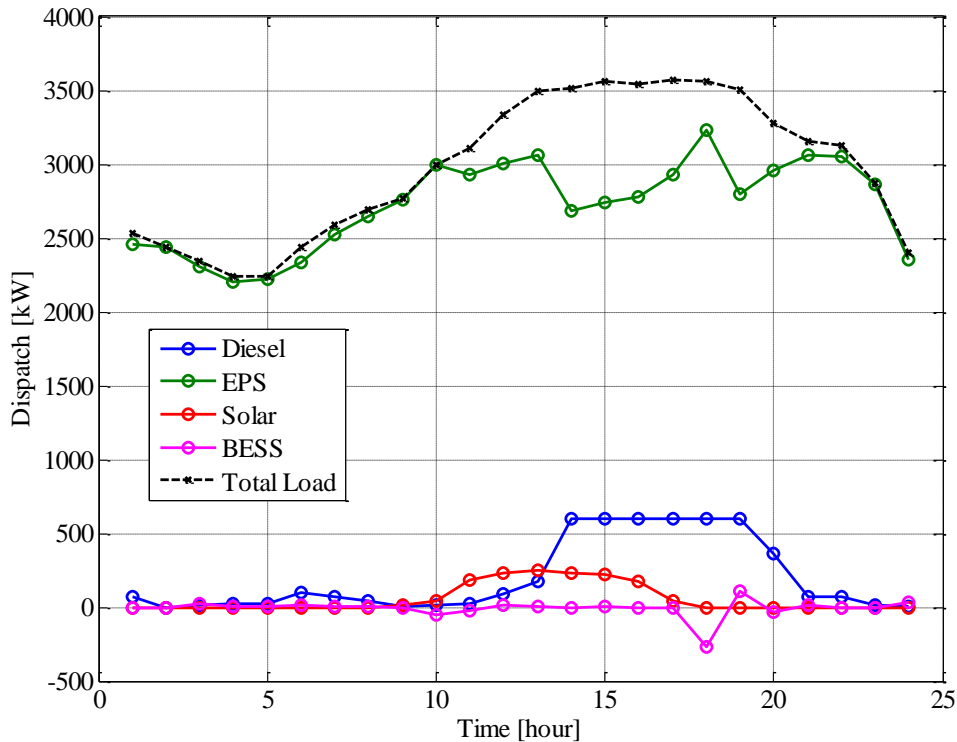


Fig. 3.8 Hourly dispatch values for case shown in Fig. 3.7.

For the cost objective, the curve follows around 1.0 and over-achievement of the goal is attained by decrease in import from EPS due to solar output, and in turn an increase in 14th hour

due to increase in the output of diesel generator. This occurs in form of over-achieving the cost objective at 12th hour and returning to close to the goal in 13th hour. This is due to the two-hour look ahead and this decision is made based on the overall minimum cost calculated over t , $t+1$, and $t+2$ hours. The diesel generator stays on during two scenarios till 19th hour to support the load reduction objective. During the start of on-peak period, solar PV output contributes positively to load reduction, and cost. By 18th hour, solar PV output goes to zero, and hence at 19th hour, the contribution from solar is reduced which is evident in the under-achievement of load reduction despite high output of diesel generator. The emission objective is under-achieved during all hours due to a very aggressive goal of 30% reduction over base emission. This effect is not just affected by the goal, but the preference weights relative to the other objectives. Most reduction occurs by virtue of solar PV output. To clearly show the dispatch values of battery, solar PV, and diesel generator the stacked bar chart is shown in Fig. 3.9.

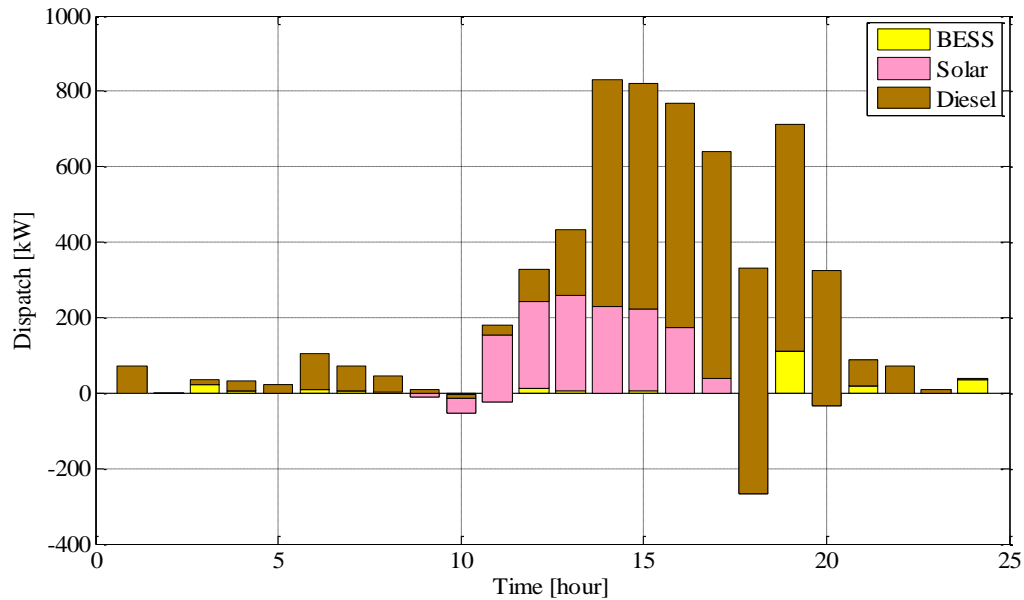


Fig. 3.9 Bar chart (stacked) for hourly dispatch values for battery, PV, and diesel generator

To see the overall effect of the decision-making on the objectives, average values of objective functions in per unit for stochastic and deterministic dispatch are listed in Table 3.3.

These solutions correspond to goals, preference weights, and MCDA selection for five representative scenarios. Thus, the presented example above is a microgrid operation aimed at load reduction during on-peak hours, and the preference weights represent the same. The close attainment of the goals shows the effectiveness of the method. A DSO with a different preference for the three objectives may formulate and run the dispatch optimization and MCDA differently. Also, while checking the voltage constraint in RSCAD[®], the MCDA chooses the next ranked solutions for dispatch in case of infeasibility. An alternative will be to provide corrections to the voltage excursions through reactive power compensation; but, that is a design solution and it is not explored here as we are concerned with the dispatch problem. During the simulations in RSCAD[®] no overvoltage occurred at any node for rank-1 solutions. In case of an overvoltage, the next ranked solution is chosen iteratively until the voltages are found to be within limits. For MCDA process, L^∞ norm was used as the measure of closeness and the choice for ranking.

Table 3.3 Objective function average values for scenario-based and deterministic dispatch

	24 hour	On-peak	Off-peak
$\widetilde{\varphi}_1$	1.0005	0.9549	1.3932
$\widetilde{\varphi}_2$	0.9773	1.0085	0.9668
$\widetilde{\varphi}_3$	1.3932	1.3661	1.4022
φ_1	1.0075	0.9214	1.0363
φ_2	0.9486	0.9630	1.3183
φ_3	1.0363	0.9438	1.3880

For the purposes of MCDA, the most ideal and least ideal values for each objective are identified among the given alternatives. This is done each hour considering the two hour look-ahead approach. This generates 125 alternatives which are not shown to the DM. The reason is

that for a larger case of multiple dispatchable and non-dispatchable DERs can have many more feasible alternatives which can make the decision making process non-trivial. The simple microgrid case presented here consists of three DERs and still the choice is 125 sets of alternatives with each containing three objective function values. Even for a simple case presented here, the intuitive tradeoff is a non-trivial task. This becomes more arduous as the complexity of the system increases with more variables, objectives, and constraints. This reiterates the necessity of a systematic process such as MCDA for obtaining a trade-off amongst given alternatives. The DM preference weights given by ω are applied for MCDA after identifying the best-achievable (φ_{best}) and worst-achievable (φ_{worst}) sets. These sets act as references for calculation of norm distance given by (7). A sample case is shown in Table 3.4 below for simulation of a scenario during 19th hour. The total *cost-to-go* function is calculated as sum of three objective function values over t, t+1, and t+2.

Table 3.4. MCDA process for selection of dispatch corresponding to minimum cost-to-go function during 19th hour

Preference weights, $\omega = [10, 100, 1]$		$\varphi_{worst} = [3.4074, -0.1238, 3.0346]$ $\varphi_{best} = [2.9272, -0.3681, 2.9144]$	
		Cost-to-go	Objective value
Top-ranking	φ_1	2.9518	0.9314
solution based on	φ_2	-0.1980	-0.2189
19 th to 21 st hr <i>cost-to-go</i>	φ_3	2.9532	0.9328

It can be observed that the tradeoff amongst various objectives results in the top-ranked solution to lie somewhere between the best- and worst-achievable solutions. The most ideal and

least ideal cost-to-go values are chosen based on minimizing criteria, i.e. smallest distance of norm calculated. L^∞ -norm is used in the simulations and MCDA weights are kept same as optimization weights. However, the DM has the flexibility to choose different weights for different time periods.

Conclusions

A multi-objective optimization approach is used for day-ahead dispatch in electric microgrids considering the variability and stochasticity in renewables and load demand through scenarios. Scenario reduction technique is employed to avoid computational intractability of the stochastic optimization problem. Energy storage is scheduled in the microgrid using dynamic programming routine for two hour look-ahead dispatch. Non-commensurable and conflicting objectives are handled without aggregation. DCP-based MCDA is used for selection of non-dominated dispatch solutions at each hour that are *closest* to the preferences for the objectives as per the DM. The MCDA process is interactive as it provides the flexibility to the DM for revising the preferences to obtain a satisfactory solution. Feasibility is ensured for the generated solutions through physical constraint testing in RSCAD[®] microgrid model. This approach provides non-dominated solutions without generating a Pareto front. The presented approach is general enough to be implemented in any microgrid with a different configuration and functionalities than the ones presented here, and can be used by DSO as a DSS in actual system operation.

REFERENCES FOR CHAPTER-3

- [3.1] S. A. Soliman, A. H. Mantawy, “Economic Dispatch (ED) and Unit Commitment Problems (UCP): Formulation and Solution Algorithms,” in *Modern Optimization Techniques with Applications in Electric Power Systems*, Energy Systems, Springer, 2012, pp. 185-279.
- [3.2] G. T. Heydt, *Computer Analysis Methods for Power Systems*. MacMillan Press Ltd., London, UK, 1986.
- [3.3] J. H. Talaq, F. El-Hawary, and M. E. El-Hawary, “A summary of environmental/economic dispatch algorithms,” *IEEE Transactions on Power Systems*, vol. 9, no. 3, pp. 1508–1516, Aug. 1994.
- [3.4] D. B. Das and C. Patvardhan, “New multi-objective stochastic search technique for economic load dispatch,” *Generation, Transmission and Distribution, IEE Proceedings*-, vol. 145, no. 6, pp. 747–752, Nov. 1998.
- [3.5] P. P. Varaiya, F. F. Wu, and J. W. Bialek, “Smart Operation of Smart Grid: Risk-Limiting Dispatch,” *Proceedings of the IEEE*, vol. 99, no. 1, pp. 40–57, Jan. 2011.
- [3.6] B. Zhou, K. W. Chan, T. Yu, and C. Y. Chung, “Equilibrium-Inspired Multiple Group Search Optimization With Synergistic Learning for Multiobjective Electric Power Dispatch,” *IEEE Transactions on Power Systems*, vol. 28, no. 4, pp. 3534–3545, Nov. 2013.
- [3.7] Q. Jiang, M. Xue, and G. Geng, “Energy Management of Microgrid in Grid-Connected and Stand-Alone Modes,” *IEEE Transactions on Power Systems*, vol. 28, no. 3, pp. 3380–3389, Aug. 2013.
- [3.8] W.-T. Huang, K.-C. Yao, and C.-C. Wu, “Using the Direct Search Method for Optimal Dispatch of Distributed Generation in a Medium-Voltage Microgrid,” *Energies*, vol. 7, no. 12, pp. 8355–8373, Dec. 2014.
- [3.9] Smart Grid Demonstration Program. [Online]. Available: https://www.smartgrid.gov/recovery_act/overview/smart_grid_demonstration_program.html.
- [3.10] D. T. Ton and M. A. Smith, “The U.S. Department of Energy’s Microgrid Initiative,” *The Electricity Journal*, vol. 25, no. 8, pp. 84–94, Oct. 2012.
- [3.11] The role of microgrids in helping to advance the nation’s energy system. [Online]. Available: <http://energy.gov/oe/services/technology-development/smart-grid/role-microgrids-helping-advance-nation-s-energy-system>.
- [3.12] IEEE Guide for Design, Operation, and Integration of Distributed Resource Island Systems with Electric Power Systems, IEEE Std 1547.4-2011, 2011.

- [3.13] CERTS Microgrid Definitions. [Online] Available: <https://building-microgrid.lbl.gov/microgrid-definitions>
- [3.14] N. Hatziargyriou, H. Asano, R. Iravani, and C. Marnay, "Microgrids," *IEEE Power and Energy Magazine*, vol. 5, no. 4, pp. 78–94, Jul. 2007.
- [3.15] C. Schwaegerl, L. Tao, "Quantification of Technical, Economic, Environmental and Social Benefits of Microgrid Operation," in N. Hatziargyriou, editor, *Microgrids: Architectures and Control*, Wiley-IEEE Press, 2014, pp.344.
- [3.16] S. Suryanarayanan, F. Mancilla-David, J. Mitra, and Y. Li, "Achieving the Smart Grid through customer-driven microgrids supported by energy storage," in *2010 IEEE International Conference on Industrial Technology (ICIT)*, 2010, pp. 884–890.
- [3.17] C. Abbey, D. Cornforth, N. Hatziargyriou, K. Hirose, A. Kwasinski, E. Kyriakides, G. Platt, L. Reyes, and S. Suryanarayanan, "Powering Through the Storm: Microgrids Operation for More Efficient Disaster Recovery," *IEEE Power and Energy Magazine*, vol. 12, no. 3, pp. 67–76, May 2014.
- [3.18] S. Parhizi, H. Lotfi, A. Khodaei, and S. Bahramirad, "State of the Art in Research on Microgrids: A Review," *IEEE Access*, vol. 3, pp. 890–925, 2015.
- [3.19] S. Chowdhury, S. P. Chowdhury, and P. Crossley, *Microgrids and Active Distribution Networks*. IET Digital Library, 2009.
- [3.20] M. A. Abido, "Multiobjective evolutionary algorithms for electric power dispatch problem," *IEEE Transactions on Evolutionary Computation*, vol. 10, no. 3, pp. 315–329, Jun. 2006.
- [3.21] F. Gembicki and Y. Y. Haimes, "Approach to performance and sensitivity multiobjective optimization: The goal attainment method," *IEEE Transactions on Automatic Control*, vol. 20, no. 6, pp. 769–771, Dec. 1975.
- [3.22] B. R. Sathyanarayana and G. T. Heydt, "A roadmap for distribution energy management via multiobjective optimization," in *2010 IEEE Power and Energy Society General Meeting*, 2010, pp. 1–8.
- [3.23] K.-H. Kim, S.-B. Rhee, K.-B. Song, and K. Y. Lee, "An efficient operation of a micro grid using heuristic optimization techniques: Harmony search algorithm, PSO, and GA," in *2012 IEEE Power and Energy Society General Meeting*, 2012, pp. 1–6.
- [3.24] Y. V. Makarov, C. Loutan, J. Ma, and P. de Mello, "Operational Impacts of Wind Generation on California Power Systems," *IEEE Transactions on Power Systems*, vol. 24, no. 2, pp. 1039–1050, May 2009.
- [3.25] Y. V. Makarov, P. V. Etingov, J. Ma, Z. Huang, and K. Subbarao, "Incorporating Uncertainty of Wind Power Generation Forecast Into Power System Operation, Dispatch,

- and Unit Commitment Procedures,” *IEEE Transactions on Sustainable Energy*, vol. 2, no. 4, pp. 433–442, Oct. 2011.
- [3.26] J. Ma, Y. V. Makarov, C. Loutan, and Z. Xie, “Impact of wind and solar generation on the California ISO’s intra-hour balancing needs,” in *2011 IEEE Power and Energy Society General Meeting*, 2011, pp. 1–6.
- [3.27] W. Su, J. Wang, and J. Roh, “Stochastic Energy Scheduling in Microgrids With Intermittent Renewable Energy Resources,” *IEEE Transactions on Smart Grid*, vol. 5, no. 4, pp. 1876–1883, Jul. 2014.
- [3.28] G. Liu, Y. Xu, and K. Tomsovic, “Bidding Strategy for Microgrid in Day-Ahead Market Based on Hybrid Stochastic/Robust Optimization,” *IEEE Transactions on Smart Grid*, vol. 7, no. 1, pp. 227–237, Jan. 2016.
- [3.29] J. M. Morales, S. Pineda, A. J. Conejo, and M. Carrion, “Scenario Reduction for Futures Market Trading in Electricity Markets,” *IEEE Transactions on Power Systems*, vol. 24, no. 2, pp. 878–888, May 2009.
- [3.30] X. Y. Ma, Y. Z. Sun, H. L. Fang, and Y. Tian, “Scenario-Based Multiobjective Decision-Making of Optimal Access Point for Wind Power Transmission Corridor in the Load Centers,” *IEEE Transactions on Sustainable Energy*, vol. 4, no. 1, pp. 229–239, Jan. 2013.
- [3.31] K. A. Baker, “Coordination of Resources Across Areas for the Integration of Renewable Generation: Operation, Sizing, and Siting of Storage Devices,” 2014.
- [3.32] A. Soroudi and T. Amraee, “Decision making under uncertainty in energy systems: State of the art,” *Renewable and Sustainable Energy Reviews*, vol. 28, pp. 376–384, Dec. 2013.
- [3.33] K. Rahbar, J. Xu, and R. Zhang, “Real-Time Energy Storage Management for Renewable Integration in Microgrid: An Off-Line Optimization Approach,” *IEEE Transactions on Smart Grid*, vol. 6, no. 1, pp. 124–134, Jan. 2015.
- [3.34] W. Shi, N. Li, C.-C. Chu, and R. Gadh, “Real-Time Energy Management in Microgrids,” *IEEE Transactions on Smart Grid*, vol. PP, no. 99, pp. 1–1, 2015.
- [3.35] T. Li and M. Dong, “Real-Time Energy Storage Management With Renewable Integration: Finite-Time Horizon Approach,” *IEEE Journal on Selected Areas in Communications*, vol. 33, no. 12, pp. 2524–2539, Dec. 2015.
- [3.36] K. Goetzmann, “The Power of Compromise Reference Point Methods and Approximation in Multicriteria Optimization,” *Ph.D. Thesis*, TU Berlin, Germany, 2012.
- [3.37] F. Ruiz, “Choosing an efficient solution: Compromise Programming, Reference Point,” *Multicriteria Decision Making with Mathematical Programming*, Complutense University and Technical University of Madrid, Spain, February 17–28, 2014. [Online]. Available: http://www.mat.ucm.es/imeio/cursos/EPS_MCDM/Documents/FRuiz1.pdf

- [3.38] D. Parra, M. Gillott, S. A. Norman, and G. S. Walker, "Optimum community energy storage system for PV energy time-shift," *Applied Energy*, vol. 137, pp. 576–587, Jan. 2015.
- [3.39] Fort Collins Utilities (FCU) Time of Use Rates Pilot Study. [Online]. Available: <http://www.fcgov.com/utilities/residential/rates/time-of-use/>
- [3.40] Y. Han, P. Young, and D. Zimmerle, "Optimal selection of generators in a microgrid for fuel usage minimization," in *2013 IEEE Power and Energy Society General Meeting (PES)*, 2013, pp. 1–5.
- [3.41] Standards of Performance for Greenhouse Gas Emissions from New, Modified, and Reconstructed Stationary Sources: Electric Utility Generating Units, EPA Rule for Clean Air Act (CAA). [Online]. Available: <http://www.epa.gov/airquality/cpp/cps-final-rule.pdf>.
- [3.42] AP 42 Compilation of Air Pollutant Emission Factors. [Online]. Available: <http://www.epa.gov/ttnchie1/ap42/ch03/final/c03s04.pdf>.
- [3.43] Energy Information Agency (EIA) Voluntary Reporting of Greenhouse Gases Program Fuel Emission Coefficients [Online]. Available: <http://www.eia.gov/oiaf/1605/coefficients.html#tbl2>
- [3.44] Y. Collette, P. Siarry, *Multiobjective Optimization Principles and Case Studies*, Decision Engineering, Springer, 2004
- [3.45] M. Basseur, E. Talbi, A. Nebro, E. Alba, "Metaheuristics for multiobjective combinatorial optimization problems: Review and recent issues," INRIA Report, 2006.
- [3.46] W. H. Kersting, "Distribution Feeder Voltage Regulation Control," *IEEE Transactions on Industry Applications*, vol. 46, no. 2, pp. 620–626, Mar. 2010.
- [3.47] W. H. Kersting, "Radial distribution test feeders," in *Proc. 2001 IEEE Power Engineering Society Winter Meeting*, pp. 908-912, 2001.
- [3.48] K. Mentesidi, E. Rikos, V. Kleftakis, P. Kotsampopoulos, M. Santamaria, and M. Aguado, "Implementation of a microgrid model for DER integration in real-time simulation platform," in *2014 IEEE 23rd International Symposium on Industrial Electronics (ISIE)*, 2014, pp. 2274–2279.
- [3.49] J. Han, J. Prigmore, Z. Wang, and S. Khushalani-Solanki, "Modeling and coordinated controller design of a microgrid system in RTDS," in *2013 IEEE Power and Energy Society General Meeting (PES)*, 2013, pp. 1–5.
- [3.50] O. Nzimako and R. Wierckx, "Modeling and simulation of a grid-integrated photovoltaic system using a real-time digital simulator," in *Power Systems Conference (PSC), 2015 Clemson University*, 2015, pp. 1–8.

- [3.51] A. Yazdani and P. P. Dash, “A Control Methodology and Characterization of Dynamics for a Photovoltaic (PV) System Interfaced With a Distribution Network,” *IEEE Transactions on Power Delivery*, vol. 24, no. 3, pp. 1538–1551, Jul. 2009.
- [3.52] I. U. Nutkani, P. C. Loh, P. Wang, and F. Blaabjerg, “Decentralized Economic Dispatch Scheme With Online Power Reserve for Microgrids,” *IEEE Transactions on Smart Grid*, vol. PP, no. 99, pp. 1–1, 2015.
- [3.53] “Electric Machine Models,” in *RTDS Power System User’s Manual*, RTDS Technologies
- [3.54] “VSC Small Time-Step Modeling,” in *RTDS Manuals*, RTDS Technologies
- [3.55] Fort Collins Weather Station Data, Colorado State University, Ft. Collins, CO, U.S.A. [Online]. Available: http://climate.colostate.edu/~autowx/fclwx_access.php. Last Accessed: 08/24/2015.
- [3.56] U.S. On-Highway Diesel Fuel Prices. [Online]. Available: <http://www.eia.gov/petroleum/gasdiesel/>.
- [3.57] PRPA load curve. [Online]. Available: <http://www.prpa.org/load/load.htm>.
- [3.58] M. Panwar, S. Suryanarayanan, and S. Chakraborty, “Steady-state modeling and simulation of a distribution feeder with distributed energy resources in a real-time digital simulation environment,” in *North American Power Symposium (NAPS), 2014*, 2014, pp. 1–6.

CHAPTER 4

PERFORMANCE METRICS FOR RESERVE MANAGEMENT

4.1 Performance Metrics

Electric microgrids consist of DERs that are inherently different in terms of dispatchability from traditional power system generators such as nuclear or coal-fired thermal or hydroelectric generators³. Performance of traditional electric power grid generators is measured using NERC metrics. Some of the NERC metrics can be used to quantify the performance of dispatchable and non-dispatchable DERs in the microgrid [4.1]. The inherent variability in the electric power output of non-dispatchable DERs and inability to accurately forecast the output poses risk to power system scheduling and dispatch. Capacity reserves in the microgrid become a crucial measure to mitigate the risk. Reserves management in traditional grid is done as a heuristic such as a constant percentage based on load demand [4.2]. Traditional dispatch and reserve management does not consider performance as a criteria for operation. Therefore, the concept of using performance metrics in operation of microgrids is proposed, and reserve management in grid-connected mode of operation is chosen as an area of application of performance metrics. This requires some new performance metrics specific to application to reserve management. We apply some NERC metrics to quantify reliability of microgrid assets and incorporate these with other factors in the microgrid such as load demand, capacity rating, and power output of the non-dispatchable and dispatchable assets. All of the abovementioned factors are used to formulate a

³Disclaimer: Chapter-4 is a verbatim reproduction of a paper under preparation for a peer-reviewed publication listed as Paper-4 in Table 1.1 of Chapter-1 in this dissertation. The required permissions for re-use of the material have been obtained from the copyright holders and are included in the Appendix. The numbering of the figures and tables has been modified to satisfy the formatting requirements of the dissertation.

performance metric to quantify the net value of reserve of the microgrid through *self-provision*. Some new performance metrics are developed that combine the traditional and previously developed metrics to assess the reliability of the grid. The characteristics of the constituent DERs are measured through traditional metrics and combined with the new performance metrics to evaluate the reliability-based cost and value of the unused reserves of the microgrid. The reliability-based metrics for reserve are then used as a constraint in the dispatch. The idea is to use performance of each asset and incorporate the measured quality into operation of the microgrid. This performance metric is applied for reserve management in day-ahead dispatch.

Reliability-based Evaluation of Reserve

We first define the quantities and nomenclature used in formulation of the metrics. These are shown for an example load demand for one time period in Figure 4.1.

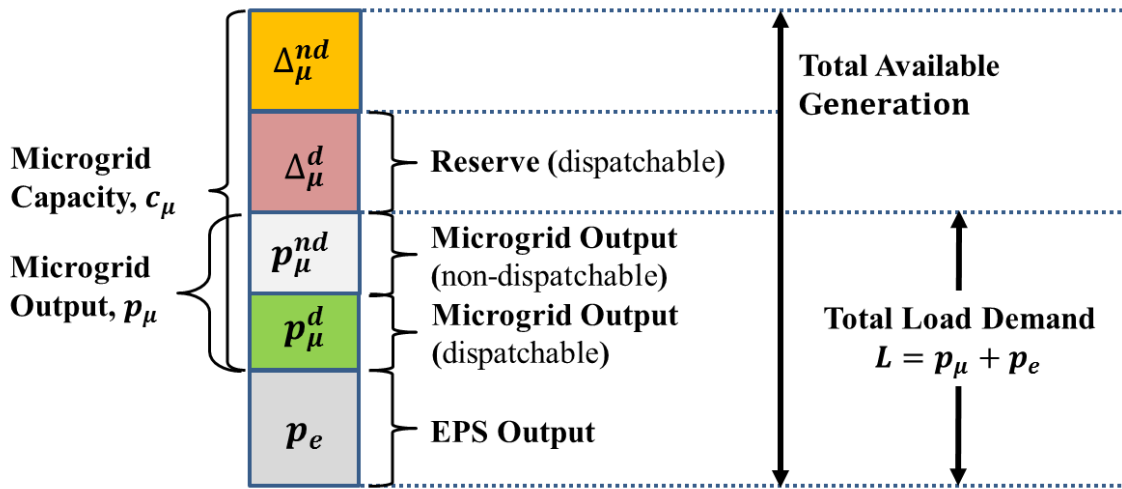


Fig. 4.1 System level representation of various capacity based quantities for one time period

Some of the previously developed metrics are used from [4.1] and are given by (1) and (2).

$$\text{Peak reserve ratio, } p_{rr}(t) = \frac{\Delta\mu(t)}{p_e(t)+p_\mu(t)} \quad (1)$$

$$\text{Peak load reduction, } PLR(t) = \frac{p_{\mu}(t)}{p_e(t)+p_{\mu}(t)} \times 100\% \quad (2)$$

where t is represents time index.

Using the reserve quantities on load demand curve, we derive the value and cost of microgrid reserve as seen by the DSO, and are given by (3) and (4).

Reliability value of unused reserve ($rvur$) in kW

$$rvur = \Delta_{\mu}^d \left[\frac{p_e w_e + p_{\mu} w_{\mu}}{p_e + p_{\mu}} \right] = prr^d [p_e w_e + p_{\mu} w_{\mu}] \text{ kW} \quad (3)$$

Reliability cost of unused reserve ($rcur$) in kW

$$\begin{aligned} rcur &= \Delta_{\mu}^d \left[\frac{(p_e - \Delta_{\mu}^d) w_e + p_{\mu} w_{\mu} + \Delta_{\mu}^d w_{\Delta_{\mu}^d}}{p_e + p_{\mu}} \right] \\ &= prr^d \left[(p_e - \Delta_{\mu}^d) w_e + p_{\mu} w_{\mu} + \Delta_{\mu}^d w_{\Delta_{\mu}^d} \right] \text{ kW} \end{aligned} \quad (4)$$

$$\text{where } prr^d = \frac{\Delta_{\mu}^d}{p_e + p_{\mu}},$$

$$p_{\mu} w_{\mu} = p_{\mu}^d w_{\mu}^d + p_{\mu}^{nd} w_{\mu}^{nd}, \text{ and } \Delta_{\mu} = \Delta_{\mu}^d + \Delta_{\mu}^{nd}$$

where w_e and w_{μ} represent the reliability of the EPS and microgrid, respectively. It may be noted that prr^d and Δ_{μ}^d correspond to dispatchable DERs, and is different from (1) which considers all the dispatchable and non-dispatchable DERs. Correspondingly, $w_{\Delta_{\mu}^d}$ is the reliability of the microgrid reserve. (3) and (4) depict the value and cost of microgrid reserve as seen by DSO. Value is derived as the product of microgrid reserve capacity and weighted reliability of the dispatched generation from EPS and microgrid. Cost of reserve is derived by product of microgrid reserve capacity and weighted reliability of the generation serving the load when full

capacity of microgrid is dispatched leaving no reserve from microgrid. Ideally, the weighted reliability metric can be ≤ 1.0 .

4.2 Application to Reserve Management in Day-ahead Dispatch

Reserve management is non-trivial in a heterogeneous microgrid due to the varying dispatchability associated with the constituent DERs. Traditionally, reserve is calculated based on economic and capacity criteria [4.2]. We propose an alternative method to calculate the reliability-based value of capacity reserve. One reliability metric from NERC, and other previously developed metrics are used for quantifying this new value [4.3], [4.4]. Reliability is quantified for the dispatched power and dispatchable reserve. Metrics $rvur$ and $rcur$ are shown in (3) and (4). $rvur$ signifies the minimum acceptable level of reliability-weighted capacity measure for equivalent reserve. $rcur$ signifies the reliability-weighted cost of using the full capacity of microgrid, i.e., zero reserve. This is a limiting case where the minimum reserve capacity can be assigned heuristically and affects $rcur$. Fig. 1 shows the relationship of the above-mentioned metrics for a typical grid-connected operation mode of a microgrid.

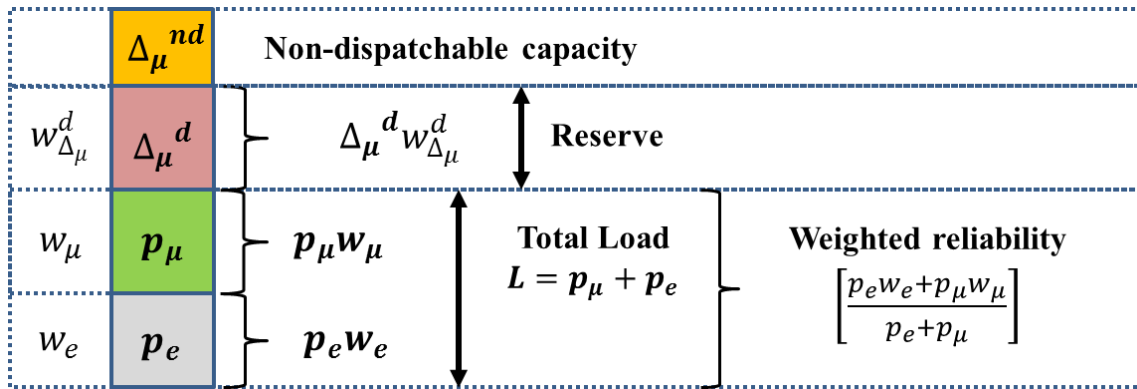


Fig. 4.2. A bar graph for microgrid operation with microgrid capacity reserve

Here, both the electric power system (EPS) and the microgrid assets serve the constituent load in the microgrid. Such an energy management decision will occur in a typical economic dispatch (ED) considering operational costs. In the islanded mode operation of the microgrid, an

appropriate reference reliability measure can be assigned instead of w_e , and applied similar to grid-connected mode. The focus of this work is grid-connected mode of operation since microgrid is expected to operate in this mode for majority of the time. Dispatch can also include peak load reduction, emissions, reliability, and other operator-defined criterion. Under such cases, reserve management can be even more challenging. Therefore, a systematic approach is required to capture the performance capability of the microgrid to mitigate the risk posed by the inherent variability of non-dispatchable DER during dispatch and scheduling. Instead of relying completely on the EPS to mitigate this risk, the concept of *self-provision* of reserves locally from microgrid DERs is used. We calculate the change in net value of reliability that can occur by utilizing all the microgrid assets. This is given in (5) as the difference of (3) and (4).

$$R = prr^d \left[\Delta_{\mu}^d w_e - \Delta_{\mu}^d w_{\Delta_{\mu}}^d \right] \text{ kW} \quad (5)$$

From Fig. 4.1 we have, $c_{\mu}^d = p_{\mu}^d + \Delta_{\mu}^d$ and $L = p_{\mu} + p_e$; by substituting in (5) and rearranging the terms, we get

$$R = \frac{(c_{\mu}^d - p_{\mu}^d)^2 [w_e - w_{\Delta_{\mu}}^d]}{L}.$$

Extrema of R provide the lower and upper bounds on R . For a minimum capacity reserve assigned heuristically, say Δ_{min} , and assuming $[w_e - w_{\Delta_{\mu}}^d] > 0$, $\min(R) = \frac{(\Delta_{min})^2 [w_e - w_{\Delta_{\mu}}^d]}{L}$, and $\max(R) = \frac{(c_{\mu}^d)^2 [w_e - w_{\Delta_{\mu}}^d]}{L}$. A threshold of 20% reserve capacity is used here in simulations, which signifies the error in solar forecasting and is a typical *rule-of-thumb* in EPS [4.5]. The formula for the NERC metric Net Output factor (NOF) used as w for the EPS and microgrid DERs are shown in (6).

$$NOF = \frac{\sum_{i=1}^{t_{period}} p_{\mu}^{d,nd} t_i}{c_{\mu}^{d,nd} \times t_{period}} \times 100\% \quad (6)$$

Typical values of NOF for EPS, dispatchable DER, and non-dispatchable DER are 81.5, 52.1, and 40.3 respectively [4.3], [4.4].

Economic Dispatch

Simulations are performed on a notional microgrid with a diesel generator (dispatchable) and a solar photovoltaic DER (non-dispatchable), of 200 kW rating each. ED is formulated as shown in (7a) and (7b).

$$\text{minimize } (f_{\mu}^d p_{\mu}^d + ToUp_e) \quad (7a)$$

$$\text{s.t. } -\Delta_{\mu}^d \leq -\Delta_{min}, 0 \leq p_{\mu}^d \leq c_{\mu}^d, p_{\mu} + p_e = L \quad (7b)$$

Power-flow constraints are not considered, but can be included without loss of generality. The cost function of dispatchable diesel is $f_{\mu}^d = 7.5992(p_{\mu}^d/c_{\mu}^d)^2 + 26.0886(p_{\mu}^d/c_{\mu}^d) + 6.3506$ [5]; the time-of-use (ToU) price is 0.2202 \$/kWh for 14th to 19th hour, and 0.0624 \$/kWh otherwise for the EPS [4.7]. The load demand curve is taken from [4.8] and linearly scaled by a factor of 10^{-3} (from MW to kW values). Solar irradiance and temperature data are taken from [4.9]. The simulation data are shown in Table 4.1.

Table 4.1 Data for load demand and solar output

Hour (h)	L (kW)	p_{μ}^{nd} (kW)
1	328	0
2	310	0
3	299	0
4	285	0
5	296	0
6	307	0
7	330	3.89
8	350	40.97
9	371	79.31
10	392	123.71
11	413	155.32
12	433	179.49
13	445	191.98
14	453	187.29
15	462	179.66
16	468	154.20
17	477	121.02
18	477	81.15
19	458	36.79
20	436	4.87
21	430	0
22	413	0
23	376	0
24	340	0

$$p_{\mu}^{nd} = c_{\mu}^{nd} \frac{S_{irr}}{S_{stm}} [1 + k(T_c - T_r)], \quad \text{where } S_{irr} \text{ is the solar irradiance in W/m}^2; S_{stm} = 1000$$

W/m²; $k = -0.0046$; $T_c = 25^{\circ}\text{C}$, and T_r is temperature of solar array.

Table 4.2 shows the average hourly cost for various cases of capacity reserves maintained during the ED. EPS-only case represents no use of DERs and has an average hourly cost of \$42.68. The values of R and the weighted reliabilities are calculated post-ED. This shows the behavior of R-metric in a classical ED setup.

Table 4.2 Economic dispatch with various capacity reserve constraints

Case	Δ_{min}	ED (\$/h)	R (kW)	Weighted reliability p.u.	
				Dispatch	Reserve
1	No constraint	37.45	78.33	0.77	-
2	20% of c_{μ}^d	37.66	79.32	0.78	0.52
3	20% of L	38.18	83.68	0.79	0.52
4	20% of p_{μ}^{nd}	37.57	78.85	0.78	0.52

Case-1 is a classical ED without any reserve constraints. Cases 2-4 represent reserve constraints as 20% of c_{μ}^d , L , and p_{μ}^{nd} respectively, and are base cases for comparison with ED using R-metric constraint. The weighted reliability of the reserve is same in all cases due to the presence of a single dispatchable DER as shown in Table 4.2. This is a capacity weighted reliability quantity and can change in case of multiple dispatchable DERs. Table 4.3 shows the ED with R-metric as L.H.S. of the constraint (7b) with Δ_{min} same as in cases 2-4. So, the constraint (7b) can be modified as

$$-R \leq -\Delta_{min}, 0 \leq p_{\mu}^d \leq c_{\mu}^d, p_{\mu} + p_e = L \quad (7c)$$

Table 4.3 Economic dispatch with R-metric as L.H.S. of reserve constraint (7c)

Case	Δ_{min}	ED (\$/h)	R (kW)	Weighted reliability p.u.	
				Dispatch	Reserve
5	20% of c_{μ}^d	38.68	88.33	0.80	0.52
6	20% of L	39.85	101.35	0.81	0.52
7	20% of p_{μ}^{nd}	38.25	84.66	0.79	0.52

A higher value of R is desirable, and the net value indicates the potential equivalent capacity available between the load serving capacity and dispatchable reserve. Case-4 (and Case-7) represents the most practical microgrid constraint scenario where the reserve corresponds to the risk posed by the variability of non-dispatchable DER [4.5]. The 24-hour dispatch for Case-7 is shown in Fig. 4.2 and the variation of R-metric and risk capacity for (7c) is shown in Fig. 4.3.

The average power output, reserve, and reserve increase for 24-hour are shown in Table 4.4.

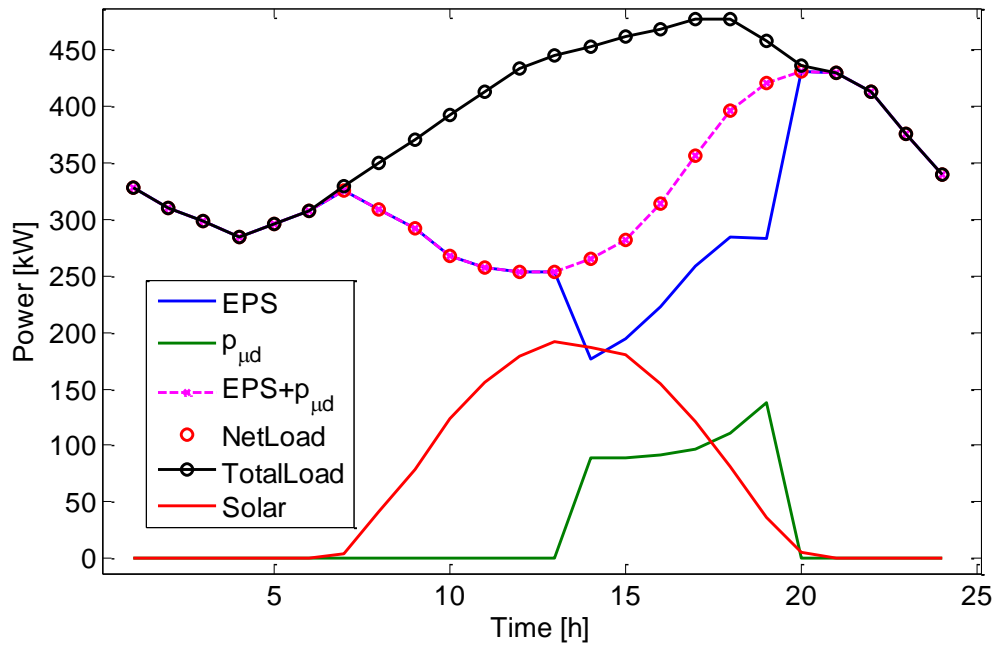


Fig. 4.3. Dispatch for Case-7 using R-metric as reserve constraint

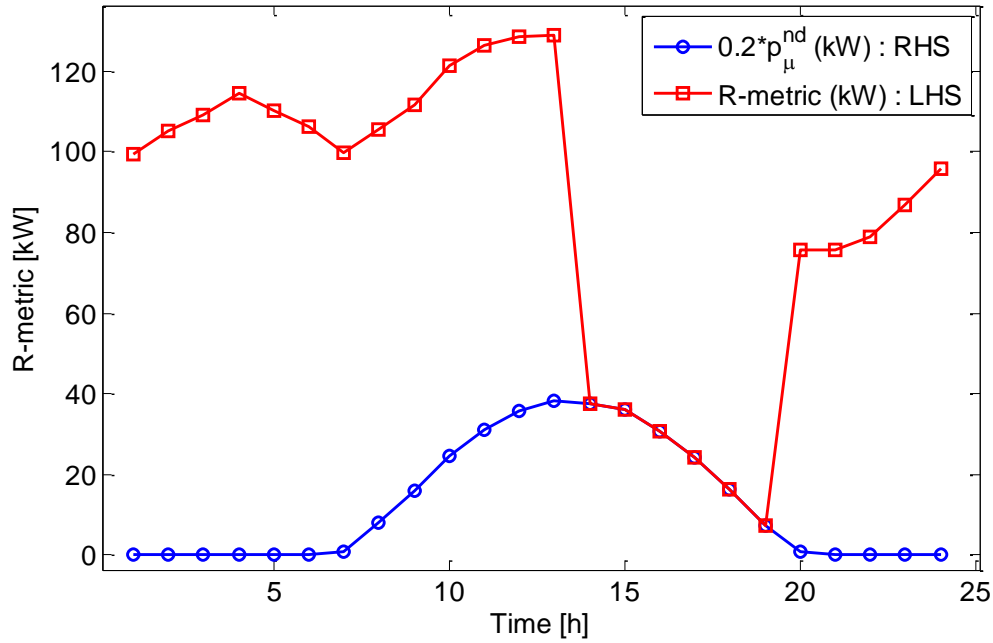


Fig. 4.4. Variation of R-metric as reserve constraint in Case-7

Table 4.4 Comparison of average dispatch and reserve values

Case	p_e (kW)	p_μ^d (kW)	Δ_μ^d (kW)	% increase in (Δ_μ^d , cost)
2	285.39	40.00	160.00	13.84, 2.71
5	307.53	17.86	182.14	
3	298.68	26.71	173.29	14.73, 4.36
6	324.20	1.19	198.81	
4	281.72	43.67	156.33	11.52, 1.80
7	299.74	25.65	174.35	

The average dispatched capacity from the microgrid DERs is lower and scheduled reserve is higher in cases 5-7, as compared to cases 2-4. Value of dispatch reliability is also higher, which is attained by importing more power from EPS, and hence the higher cost of operation. Since the reserve is provided by the microgrid assets, the EPS has an additional available

capacity equal to the risk, i.e., $\Delta_{min} = 0.2 \times p_{\mu}^{nd}$. The average value of this additional capacity over 24-hours can be 12.8303 kW. The advantage of using the new developed metric, R , is that the reserve constraint considers the reliability and performance measures that are indicative of quality of the constituent assets, both dispatchable and non-dispatchable.

4.3 Sensitivity Analysis

Sensitivity analysis is performed through ED simulations by varying the NOF for EPS, dispatchable DER, PV, and Δ_{min} , i.e., R.H.S. of (7c). The range for variations is based on typical values of each asset and heuristics [1, 3-5]. The variation is done in steps of 5%. NOF variation range for: EPS is [65%, 95%], diesel generator is [35%, 65%], and PV is [35%, 55%]. Δ_{min} variation is [5%, 30%] of p_{μ}^{nd} in steps of 5%. The results are plotted for 24-hour average for operating cost (in \$/h), R-metric (in kW), and Δ_{μ}^d (in kW) using different Δ_{min} , and are shown in Fig. 4.5. It can be observed that for a particular risk in (7c), a higher cost results in a higher reserve capacity, but a lower R-metric value. This trend is consistent in all cases with varying magnitudes of variation. Thus, it is observed that R-metric has an inverse dependence with cost and the inverse effect increases (higher slope) as Δ_{min} increases. The dispatchable reserve also has an inverse relationship with R-metric. Therefore, a higher value of desired R-metric will result in lower reserve Δ_{μ}^d . Cost and reserve have a proportional (almost linear) relationship.

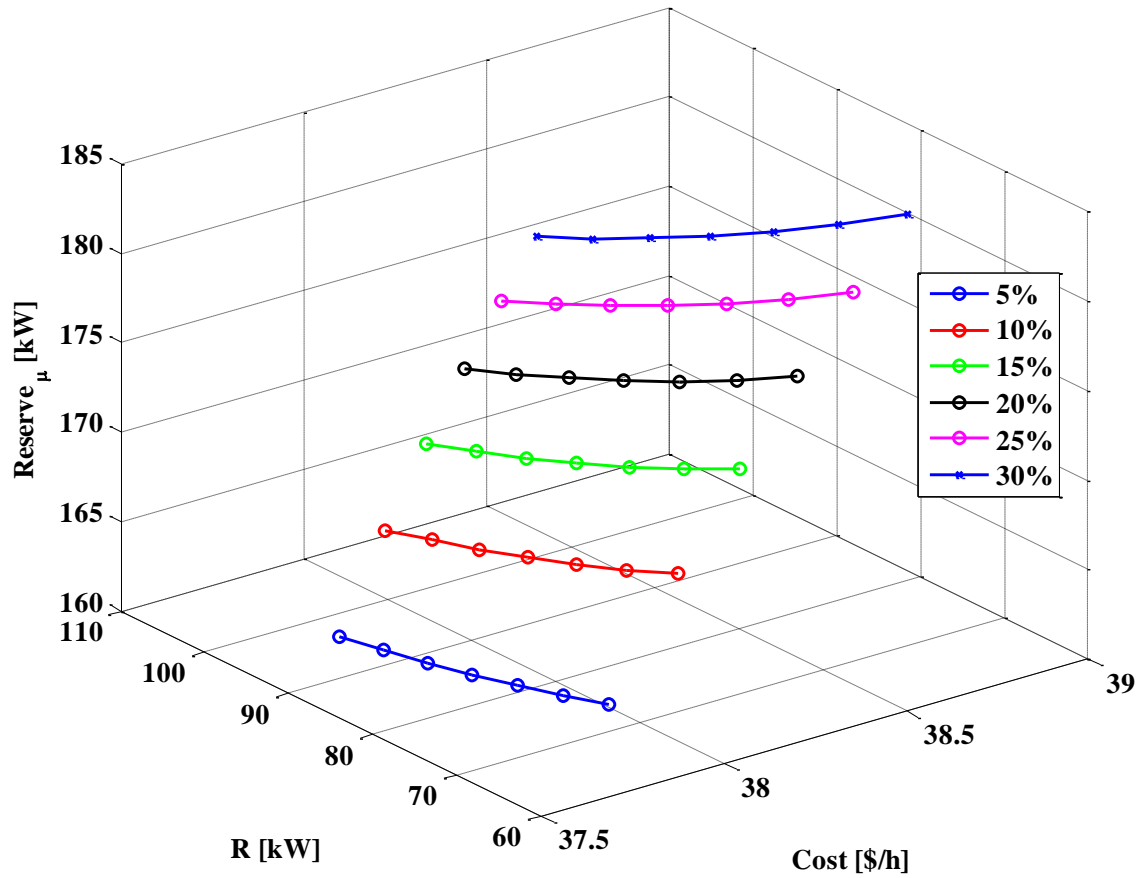


Fig. 4.5. Sensitivity analysis for R-metric

Conclusions

The formulation and application of R-metric as a constraint in day-ahead economic dispatch is presented. Sensitivity analysis shows the relationship between major interacting variables and functions such as cost, reserves etc. The inverse dependence of R-metric with cost shows that higher level of R-metric is preferable while minimizing cost in ED. Powerflow constraints are not considered for showing applicability on a simple system. Larger and more complex systems with system constraints can be included in ED as future work. Multiple objectives such as load reduction can be included in the ED in future.

REFERENCES FOR CHAPTER-4

- [4.1] M. Panwar, “Reliability quantification and visualization for electric microgrids,” M.S. thesis, Dept. Elect. and Comp. Eng., Colorado State Univ., Fort Collins, CO, 2012.
- [4.2] J. F. Prada and M. D. Ilic, “Pricing reliability: A probabilistic approach,” Large Engineering Systems Conference on Power Engineering, 1999.
- [4.3] NERC Generating Unit Statistical Brochure 2007, October 2008.
- [4.4] M. Panwar, D. Zimmerle, and S. Suryanarayanan, “Data Analysis and Visualization for Electric Microgrids: A Case Study on the FortZED RDSI Microgrid,” in *2013 IEEE Green Technologies Conference*, 2013, pp. 330–337.
- [4.5] S. Letendre, M. Makhyoun, M. Taylor, “Predicting Solar Power Production: Irradiance Forecasting Models, Applications and Future Prospects,” Solar Electric Power Association, Washington, DC, 2014.
- [4.6] Y. Han, P. Young, and D. Zimmerle, “Optimal selection of generators in a microgrid for fuel usage minimization,” in *2013 IEEE Power and Energy Society General Meeting (PES)*, 2013, pp. 1–5.
- [4.7] Fort Collins Utilities Time-of-Use rates, Online, Available: <http://goo.gl/RTv9tF>. (Accessed on August 2015).
- [4.8] PRPA Load Demand Curve, August 19, 2015, <http://www.prpa.org/load/load.htm>. (Accessed on August 2015).
- [4.9] Fort Collins Weather Station Data, Colorado State University, Ft. Collins, CO, U.S.A. Online, Available: <http://goo.gl/byOvVs>. (Accessed on May 10, 2016).

CHAPTER 5

CONCLUSIONS AND FUTURE WORK

Conclusion

The contributions of the work presented in this dissertation can be summarized in three categories as shown below.

(i) Modeling and validation of distribution test feeder in real-time simulation environment

Detailed steps for accurate modeling of the IEEE standard 13-node feeder were presented in a real-time simulation environment. This modeled system offers a good test system for simulation-based experimentation as it represents a small, but heavily loaded distribution grid. Steady-state validation results are given for voltage and phase angle deviations compared to the original test feeder document as a reference. The platform specific issues and approaches for modeling and validation are also presented to help the researchers quickly overcome the time-consuming process of troubleshooting. The model is built in RTDS-RSCAD[®] and can be used in hardware-in-the-loop experimentation. DERs are integrated to the feeder to form a microgrid capable of serving part of the load. These models are used in the simulations for dispatch in the microgrid. The model will be available for public research as part of United States DOE Grid Modernization initiative in form of an open source library [GMLC Open Library/Transient Network Project website <http://www.gmlc-ol.org/gmlc-ol>].

(ii) Day-ahead dispatch under uncertainty

A day-ahead dispatch algorithm is presented with a framework to include multiple objectives. A constrained optimization problem is solved by including physical asset-level and

system-level constraints. A diesel generator, solar photovoltaic, and battery energy storage are the constituent DERs considered in the simulations. Uncertainties due to forecasting errors of solar irradiance and load demand are included in the dispatch by using empirical distributions. Hourly data from real-world system are used for the inputs to the simulations. Stochastic scenarios are generated using samples from empirical distributions of solar irradiance and load demand values. Scenario reduction is used for maintaining computational tractability of the problem. The DM has the flexibility to include user-defined objectives or constraints, and also include the preferences of the objectives in the dispatch process. An MCDA based approach is used to help the DM choose feasible solutions that are closest to the preferences specified by the DM. The advantage of using DCP is that non-dominated solutions can be chosen without generating the computationally expensive *Pareto front*. This algorithm is implemented in MATLAB[®] and interfaced with a power grid model in RSCAD[®]. In conclusion, the decision-making process can be performed by the DSO without generating a *Pareto front*, while considering the varying preferences in the multi-objective dispatch. This approach also provides flexibility to the DM to revise preferences during MCDA.

(iii) Performance metrics for reserve management

Some new performance metrics are proposed for application in operation of microgrids. The metrics consider the performance of assets based on historical data, and associated NERC and other previously developed metrics. Use of traditional metrics such as NERC-criterion enables comparison of a traditional and non-traditional asset. An application of the developed metric is shown for reserve management in day-ahead dispatch of microgrids. Systematic inclusion of the metric in economic dispatch problem is presented. Use of reliability-based evaluation of DERs helps formulate an alternative technique to plan capacity based reserves in

microgrid. The application presented considers only one traditional measure of reliability; but based on the target applications more such traditional and user defined metrics can be included to capture multiple features of value assessment of each DER. In conclusion, the R-metric sensitivity analysis shows an inverse dependence with average operating cost. A higher value of R-metric is favorable and R has an inverse relationship with reserves, i.e., higher R-metric corresponds to lower reserves.

Future Work

Based on the work presented, potential for development lies in the area of performance metrics and decision-making for operation at smaller time-scales. More metrics can be formulated using proper aggregation techniques, such as using fuzzy measures. The composite metrics can be representative of multi-faceted (e.g., various NERC reliability metrics capturing capacity-based reliability, and successful start of a generator) value of constituent DERs. In some cases, certain mathematical properties such as convexity of the performance metric may be helpful in their inclusion in traditional optimization problems for electric microgrid power systems. For large number of assets, such properties may be exploited during optimization. Treatment of risk posed by uncertainty of constituent assets at different timescales and operational scenarios is an important area to consider while developing new performance metrics. Economics associated with assets can be integrated with the performance metric and a composite measure can be used for bidding in electricity markets. Decision-making process can be applied in a centralized or distributed framework using accurate valuation of an asset based on its inherent characteristics, location in the network, while considering composite metrics that capture economic, risk, environmental, social and other factors. Performance metrics presented in this work did not consider demand response assets. This consideration may provide a good

opportunity for future work. Metrics for assessing performance of demand response assets, especially at residential levels must be integrated with mathematical models for user behavior. Eventually, the performance metrics must provide a homogenous yardstick to compare performance of multiple heterogeneous assets across the operational domain of the electric power system.

APPENDIX



RightsLink®

Home

Account Info

Help



Title: An overview of real time hardware-in-the-loop capabilities in digital simulation for electric microgrids

Conference Proceedings: North American Power Symposium (NAPS), 2013

Author: Mayank Panwar

Publisher: IEEE

Date: Sept. 2013

Copyright © 2013, IEEE

Logged in as:

Mayank Panwar

Account #:
3001062102

LOGOUT

Thesis / Dissertation Reuse

The IEEE does not require individuals working on a thesis to obtain a formal reuse license, however, you may print out this statement to be used as a permission grant:

Requirements to be followed when using any portion (e.g., figure, graph, table, or textual material) of an IEEE copyrighted paper in a thesis:

- 1) In the case of textual material (e.g., using short quotes or referring to the work within these papers) users must give full credit to the original source (author, paper, publication) followed by the IEEE copyright line © 2011 IEEE.
- 2) In the case of illustrations or tabular material, we require that the copyright line © [Year of original publication] IEEE appear prominently with each reprinted figure and/or table.
- 3) If a substantial portion of the original paper is to be used, and if you are not the senior author, also obtain the senior author's approval.

Requirements to be followed when using an entire IEEE copyrighted paper in a thesis:

- 1) The following IEEE copyright/ credit notice should be placed prominently in the references: © [year of original publication] IEEE. Reprinted, with permission, from [author names, paper title, IEEE publication title, and month/year of publication]
- 2) Only the accepted version of an IEEE copyrighted paper can be used when posting the paper or your thesis on-line.
- 3) In placing the thesis on the author's university website, please display the following message in a prominent place on the website: In reference to IEEE copyrighted material which is used with permission in this thesis, the IEEE does not endorse any of [university/educational entity's name goes here]'s products or services. Internal or personal use of this material is permitted. If interested in reprinting/republishing IEEE copyrighted material for advertising or promotional purposes or for creating new collective works for resale or redistribution, please go to http://www.ieee.org/publications_standards/publications/rights/rights_link.html to learn how to obtain a License from RightsLink.

If applicable, University Microfilms and/or ProQuest Library, or the Archives of Canada may supply single copies of the dissertation.

BACK

CLOSE WINDOW

Copyright © 2016 Copyright Clearance Center, Inc. All Rights Reserved. [Privacy statement](#). [Terms and Conditions](#). Comments? We would like to hear from you. E-mail us at customercare@copyright.com



Title: Steady-state modeling and simulation of a distribution feeder with distributed energy resources in a real-time digital simulation environment

Conference Proceedings: North American Power Symposium (NAPS), 2014

Author: Mayank Panwar

Publisher: IEEE

Date: Sept. 2014

Copyright © 2014, IEEE

Logged in as:
Mayank Panwar
Account #:
3001062102

LOGOUT

Thesis / Dissertation Reuse

The IEEE does not require individuals working on a thesis to obtain a formal reuse license, however, you may print out this statement to be used as a permission grant:

Requirements to be followed when using any portion (e.g., figure, graph, table, or textual material) of an IEEE copyrighted paper in a thesis:

- 1) In the case of textual material (e.g., using short quotes or referring to the work within these papers) users must give full credit to the original source (author, paper, publication) followed by the IEEE copyright line © 2011 IEEE.
- 2) In the case of illustrations or tabular material, we require that the copyright line © [Year of original publication] IEEE appear prominently with each reprinted figure and/or table.
- 3) If a substantial portion of the original paper is to be used, and if you are not the senior author, also obtain the senior author's approval.

Requirements to be followed when using an entire IEEE copyrighted paper in a thesis:

- 1) The following IEEE copyright/ credit notice should be placed prominently in the references: © [year of original publication] IEEE. Reprinted, with permission, from [author names, paper title, IEEE publication title, and month/year of publication]
- 2) Only the accepted version of an IEEE copyrighted paper can be used when posting the paper or your thesis on-line.
- 3) In placing the thesis on the author's university website, please display the following message in a prominent place on the website: In reference to IEEE copyrighted material which is used with permission in this thesis, the IEEE does not endorse any of [university/educational entity's name goes here]'s products or services. Internal or personal use of this material is permitted. If interested in reprinting/republishing IEEE copyrighted material for advertising or promotional purposes or for creating new collective works for resale or redistribution, please go to http://www.ieee.org/publications_standards/publications/rights/rights_link.html to learn how to obtain a License from RightsLink.

If applicable, University Microfilms and/or ProQuest Library, or the Archives of Canada may supply single copies of the dissertation.

BACK

CLOSE WINDOW